

# Fast Power Curve Approximation for Posterior Analyses

Luke Hagar\*      Nathaniel T. Stevens

*Department of Statistics & Actuarial Science  
University of Waterloo, Waterloo, ON, Canada, N2L 3G1*

## Abstract

Bayesian hypothesis testing leverages posterior probabilities, Bayes factors, or credible intervals to assess characteristics that summarize data. We propose a framework for power curve approximation with such hypothesis tests that assumes data are generated using statistical models with fixed parameters for the purposes of sample size determination. We present a fast approach to explore the sampling distribution of posterior probabilities when the conditions for the Bernstein-von Mises theorem are satisfied. We extend that approach to facilitate targeted sampling from the approximate sampling distribution of posterior probabilities for each sample size explored. These sampling distributions are used to construct power curves for various types of posterior analyses. Our resulting method for power curve approximation is orders of magnitude faster than conventional power curve estimation for Bayesian hypothesis tests. We also prove the consistency of the corresponding power estimates and sample size recommendations under certain conditions.

**Keywords:** Experimental design; interval hypotheses; low-discrepancy sequences; power analysis; the Bernstein-von Mises theorem

## 1 Introduction

### 1.1 Two-Group Hypothesis Tests

Hypothesis tests allow practitioners to compare scalar quantities  $\theta_1$  and  $\theta_2$ , where the characteristic  $\theta_j$  describes a comparison ( $j = 1$ ) or reference ( $j = 2$ ) group. These comparisons are typically facilitated using the difference between the characteristics:  $\theta_1 - \theta_2$ . In Bayesian settings, hypothesis testing is often facilitated via the posterior distribution of  $\theta_1 - \theta_2$ , and point null hypotheses are rarely considered when  $\theta_1$  and  $\theta_2$  are continuous since there must be nonzero prior probability that such hypotheses are true (Gelman et al., 2013). This paper focuses on more plausible hypotheses of the form  $H_0 : \theta_1 - \theta_2 \in (\delta_L, \delta_U)$ , where  $-\infty \leq \delta_L < \delta_U \leq \infty$ . The interval  $(\delta_L, \delta_U)$  accommodates the context of comparison. Assuming larger  $\theta_j$  values are preferred, the intervals  $(\delta_L, \delta_U) = \{(0, \infty), (-\delta, \delta), (-\delta, \infty)\}$  for some  $\delta > 0$  may be used to respectively assess whether  $\theta_1$  is superior, practically equivalent (Spiegelhalter et al., 1994, 2004), or noninferior to  $\theta_2$ .

Several Bayesian hypothesis testing methods exist. Methods based on posterior probabilities have been introduced in a variety of settings (see e.g., Berry et al. (2011); Brutti et al. (2014); Stevens and Hagar

---

\*Luke Hagar is the corresponding author and may be contacted at [lmhagar@uwaterloo.ca](mailto:lmhagar@uwaterloo.ca).

(2022)). Given data observed from two groups, the relevant posterior probability is

$$Pr(\delta_L < \theta_1 - \theta_2 < \delta_U \mid data). \quad (1)$$

The probability in (1) is compared to a conviction threshold  $0.5 \leq \gamma < 1$ . Depending on whether that probability is greater than  $\gamma$ , less than  $1 - \gamma$ , or between  $1 - \gamma$  and  $\gamma$ , one should respectively conclude  $\theta_1 - \theta_2 \in (\delta_L, \delta_U)$ , conclude  $\theta_1 - \theta_2 \notin (\delta_L, \delta_U)$ , or refrain from drawing a conclusion. Larger values of  $\gamma$  allow one to draw conclusions with more conviction.

Morey and Rouder (2011) proposed the nonoverlapping hypotheses (NOH) approach to assess the plausibility of interval hypotheses with Bayes factors (Jeffreys, 1935; Kass and Raftery, 1995). This approach directly assigns a prior distribution to the effect size considered via the hypothesis test, which is  $\theta_1 - \theta_2$  in this case. Given an interval  $(\delta_L, \delta_U)$ , complementary hypotheses  $H_0 : \theta_1 - \theta_2 \in (\delta_L, \delta_U)$  and  $H_1 : \theta_1 - \theta_2 \notin (\delta_L, \delta_U)$  are defined. The NOH Bayes factor is the ratio of the posterior odds of the hypotheses  $H_0$  and  $H_1$  to their prior odds:

$$\frac{Pr(\delta_L < \theta_1 - \theta_2 < \delta_U \mid data)}{1 - Pr(\delta_L < \theta_1 - \theta_2 < \delta_U \mid data)} \div \frac{Pr(\delta_L < \theta_1 - \theta_2 < \delta_U)}{1 - Pr(\delta_L < \theta_1 - \theta_2 < \delta_U)}. \quad (2)$$

The NOH Bayes factor provides support for  $H_0$  over  $H_1$  when its value is greater than a predetermined threshold  $K \geq 1$ . Conversely, Bayes factors less than  $K^{-1}$  provide support for  $H_1$ , and Bayes factors taking values between  $K^{-1}$  and  $K$  do not strongly favour either hypothesis.

Hypothesis testing methods with credible intervals have also been proposed (Gubbiotti and De Santis, 2011; Brutti et al., 2014; Kruschke, 2018). These methods compare the credible interval for the posterior of a univariate parameter  $\theta = \theta_1 - \theta_2$  to the interval  $(\delta_L, \delta_U)$ . A credible interval  $(L_{\theta,1-\alpha}, U_{\theta,1-\alpha})$  has coverage of  $1 - \alpha$  if  $Pr(\theta \in (L_{\theta,1-\alpha}, U_{\theta,1-\alpha}) \mid data) = 1 - \alpha$ . Since this interval is not uniquely defined, the equal-tailed credible interval or highest density interval (HDI) is often considered. The equal-tailed interval is defined such that  $Pr(\theta < L_{\theta,1-\alpha} \mid data) = Pr(\theta > U_{\theta,1-\alpha} \mid data) = 1 - \alpha/2$ , and the HDI is the narrowest credible interval with coverage  $1 - \alpha$ . Depending on whether  $(L_{\theta_1 - \theta_2, 1-\alpha}, U_{\theta_1 - \theta_2, 1-\alpha})$  lies entirely within  $(\delta_L, \delta_U)$ , entirely outside  $(\delta_L, \delta_U)$ , or partially overlaps  $(\delta_L, \delta_U)$ , one should respectively conclude  $\theta_1 - \theta_2 \in (\delta_L, \delta_U)$ , conclude  $\theta_1 - \theta_2 \notin (\delta_L, \delta_U)$ , or refrain from drawing a conclusion.

For positive characteristics  $\theta_1$  and  $\theta_2$ , the posterior of  $\theta_1/\theta_2$  facilitates two-group comparisons via percentage increases with the hypothesis  $H_0 : \theta_1/\theta_2 \in (\delta_L, \delta_U)$ . Given data observed from both groups, the relevant posterior probability is

$$Pr(\delta_L < \theta_1/\theta_2 < \delta_U \mid data). \quad (3)$$

The definitions provided earlier for NOH Bayes factors and credible intervals can similarly be extended to accommodate the posterior of  $\theta = \theta_1/\theta_2$ . Posterior probabilities are invariant to monotonic transformations, so the probability in (3) is equivalent to that from (1) when logarithmic transformations are applied to  $\theta_1$ ,  $\theta_2$ , and the interval endpoints. NOH Bayes factors and equal-tailed credible intervals are also invariant to

such transformations, but posterior HDIs are not. For ratio-based comparisons, the intervals  $(\delta_L, \delta_U) = \{(1, \infty), (\delta^{-1}, \delta)\}$  for some  $\delta > 1$  may be used to respectively assess whether  $\theta_1$  is superior or practically equivalent to  $\theta_2$ .

Because posterior probabilities are used to define Bayes factors and credible intervals, this paper emphasizes hypothesis tests facilitated via posterior probabilities. However, the methods proposed in this article accommodate hypothesis tests with interval hypotheses conducted using all three overviewed methods for Bayesian inference. This broader applicability is illustrated with less emphasis throughout the paper. To ensure one has collected enough data to reliably conclude  $\theta_1 - \theta_2 \in (\delta_L, \delta_U)$  or  $\theta_1/\theta_2 \in (\delta_L, \delta_U)$  when the corresponding hypothesis  $H_0$  is true, sample size determination is an important component of the design of Bayesian hypothesis tests.

## 1.2 Bayesian Power Analysis

Power-based approaches to Bayesian sample size determination aim for pre-experimental probabilistic control over testing procedures for the parameter of interest  $\theta$ . In pre-experimental settings, the data have not been observed and are random variables. Data from a random sample of size  $n$  are represented by  $\mathbf{Y}^{(n)}$ . For two-group comparisons,  $\mathbf{Y}^{(n)}$  may consist of  $n$  observations from each group. To implement power analysis, a sampling distribution for  $\mathbf{Y}^{(n)}$  must be specified. Typically, a *design* prior  $p_D(\theta)$  (De Santis, 2007; Berry et al., 2011; Gubbiotti and De Santis, 2011) is defined to model uncertainty regarding  $\theta$  in pre-experimental settings. Design priors are often informative and concentrated on  $\theta$  values that are relevant to the objective of the study. The design prior is rarely the same prior  $p(\theta)$  used to analyze the observed data, often called the *analysis* prior. The design prior gives rise to the prior predictive distribution of  $\mathbf{Y}^{(n)}$ :

$$p(\mathbf{y}^{(n)}) = \int p(\mathbf{y}^{(n)}|\theta)p_D(\theta)d\theta.$$

The relevant power criteria defined for the Bayesian inferential methods hold when the data are generated from this prior predictive distribution.

Gubbiotti and De Santis (2011) defined two methodologies for choosing the sampling distribution of  $\mathbf{Y}^{(n)}$ : the conditional and predictive approaches. The conditional approach fixes a *design value*  $\theta_0$  for the parameter of interest. The power criteria are then based on the probability density or mass function  $f(y; \theta_0)$ . The conditional approach is typically used in frequentist sample size calculations. The predictive approach uses a (nondegenerate) design prior  $p_D(\theta)$ , which is arguably more consistent with the Bayesian framework. However, this paper discusses advantages to using the conditional approach that may outweigh its weaknesses for certain practitioners.

Bayesian methods for power analysis have been proposed in a variety of contexts (Berry et al., 2011; Gubbiotti and De Santis, 2011; Brutti et al., 2014). In these contexts, one aims to select a sample size  $n$  to ensure the probability of concluding that  $H_0$  is true is at least  $\Gamma$  for some target power  $\Gamma \in (0, 1)$ . For

hypothesis tests with posterior probabilities, the selected sample size ensures that

$$\mathbb{E}(\mathbb{I}(Pr(\delta_L < \theta < \delta_U | \mathbf{Y}^{(n)}) \geq \gamma)) \geq \Gamma, \quad (4)$$

for some conviction threshold  $\gamma \in [0.5, 1)$ . When  $\mathbf{Y}^{(n)} \sim p(\mathbf{y}^{(n)})$ ,  $p_D(\delta_L < \theta < \delta_U)$  provides an upper bound for the attainable target power. For two-group comparisons,  $\theta = h(\theta_1, \theta_2)$  for some function  $h(\cdot)$ . This paper considers  $h(\theta_1, \theta_2) = \theta_1 - \theta_2$  and  $h(\theta_1, \theta_2) = \theta_1/\theta_2$ . The case where  $\theta = \log(\theta_1) - \log(\theta_2)$  can be viewed as a generalization of  $h(\theta_1, \theta_2) = \theta_1 - \theta_2$ . It follows from (2) that the NOH Bayes factor exceeds  $K$  if and only if

$$Pr(\delta_L < \theta < \delta_U | data) > \frac{K \times Pr(\delta_L < \theta < \delta_U)}{1 - (K - 1) \times Pr(\delta_L < \theta < \delta_U)}. \quad (5)$$

The power criterion for NOH Bayes factors with threshold  $K \geq 1$  is therefore a special case of (4) when the conviction threshold  $\gamma$  equals the right side of (5).

For hypothesis tests with credible intervals, the quantity in (4) is replaced with

$$\mathbb{E}(\mathbb{I}(L_{\theta, 1-\alpha}(\mathbf{Y}^{(n)}) > \delta_L \cap U_{\theta, 1-\alpha}(\mathbf{Y}^{(n)}) < \delta_U)) \geq \Gamma, \quad (6)$$

where the endpoints of the credible interval are henceforth denoted  $L_{\theta, 1-\alpha}(\mathbf{Y}^{(n)})$  and  $U_{\theta, 1-\alpha}(\mathbf{Y}^{(n)})$  to emphasize their dependence on the data. If the posterior credible interval is equal tailed, the power criterion in (6) simplifies to

$$\mathbb{E}(\mathbb{I}(Pr(\theta < \delta_L | \mathbf{Y}^{(n)}) < \alpha/2 \cap Pr(\theta > \delta_U | \mathbf{Y}^{(n)}) < \alpha/2)) \geq \Gamma. \quad (7)$$

When  $1 - \alpha = \gamma$ , (6) and (7) impose stricter criteria than (4). At least  $100 \times \gamma\%$  of the posterior for  $\theta$  must lie within the interval  $(\delta_L, \delta_U)$  for  $(L_{\theta, 1-\alpha}(\mathbf{Y}^{(n)}), U_{\theta, 1-\alpha}(\mathbf{Y}^{(n)}))$  to also be contained in this interval. The plot of the quantity in (4), (6), or (7) as a function of the sample size  $n$  is called the power curve.

Minimum sample sizes that satisfy power criteria can be found analytically in certain situations where conjugate priors are used (see e.g., Spiegelhalter et al. (1994); Gubbiotti and De Santis (2011)). To support more flexible study design, sample sizes that satisfy power criteria can be found using simulation. Most simulation-based procedures for power analysis with design priors follow a similar process (Wang and Gelfand, 2002). First, a sample size  $n$  is selected. Second, a value  $\tilde{\theta}$  is drawn from the design prior  $p_D(\theta)$ . Third, data  $\tilde{\mathbf{y}}^{(n)}$  are generated according to the model  $f(\mathbf{y}; \tilde{\theta})$ . Fourth, the posterior of  $\theta$  given  $\tilde{\mathbf{y}}^{(n)}$  is approximated to check if this posterior satisfies the power criterion. This process is repeated many times to determine whether the power criterion is satisfied with probability  $\Gamma$  for the selected sample size  $n$ .

These simulation-based approaches can be very computationally intensive as many posteriors must be approximated for each sample size  $n$  considered. Wang and Gelfand (2002) recommended using bisection methods or grid searches to explore sample sizes. Even when such methods circumvent the need for practitioners to choose which sample sizes  $n$  to explore, time is still wasted considering sample sizes that are excessively large or much too small to satisfy the power criterion. Moreover, practitioners must specify several inputs when designing Bayesian hypothesis tests – including the conviction threshold  $\gamma$ , interval  $(\delta_L, \delta_U)$ ,

target power  $\Gamma$ , and design and analysis priors. Certain combinations of these inputs may yield unattainable sample sizes, but it is difficult to quickly discard these designs when using traditional simulation-based methods. A fast framework for power curve approximation with posterior analyses would mitigate this issue and expedite communication between stakeholders of the study.

### 1.3 Contributions

The remainder of this article is structured as follows. We describe a food expenditure example involving the comparison of gamma tail probabilities in Section 2. This example is referenced throughout the paper to motivate the proposed methods. In Section 3, we propose a method to approximate the sampling distribution of posterior probabilities using low-dimensional conduits for the data under the conditional approach. We also prove that this approximation to the sampling distribution gives rise to consistent power estimates under certain conditions. In Section 4, we present our method for fast power curve approximation with low-discrepancy sequences. This method facilitates targeted sampling from the approximate sampling distribution of posterior probabilities and prompts consistent sample size recommendations. In Section 5, we conduct numerical studies to explore the performance of our power curve approximation method in several settings. We conclude with a discussion of extensions to this work in Section 6.

## 2 Motivating Example with Gamma Tail Probabilities

Mexico’s National Institute of Statistics and Geography conducts a biennial survey to monitor household income and expenses along with sociodemographic characteristics. We refer to this survey by its Spanish acronym ENIGH. In the ENIGH 2020 survey (INEGI, 2021), each surveyed household was assigned a socioeconomic class: lower, lower-middle, upper-middle, and upper. We use data from the lower-middle income households (the most populous class) in the Mexican state of Aguascalientes. We split the households into two groups based on the sex of the household’s main provider. Each household has a weighting factor used to include its observation between one and four times in our data set. The datum  $y_{ij}$  collected for each household  $i = 1, \dots, n_j$ ,  $j = 1, 2$  is its quarterly expenditure on food per person measured in thousands of Mexican pesos (MXN \$1000). We exclude the 0.41% of households that report zero quarterly expenditure on food to accommodate the gamma model’s positive support. This respectively yields  $n_1 = 759$  and  $n_2 = 1959$  observations in the female ( $j = 1$ ) and male ( $j = 2$ ) provider groups that are visualized in Figure 1.

Here, we compare tail probabilities for each distribution such that  $\theta_j = Pr(y_{ij} > \kappa)$ , where  $\kappa$  is a scalar value from the support of distribution  $j = 1, 2$ . The threshold of  $\kappa = 4.82$  for this example is the median quarterly food expenditure per person (in MXN \$1000) for *upper* income households in Aguascalientes after accounting for weighting factors. Thus, we use the ratio  $\theta_1/\theta_2$  to compare the probabilities that lower-middle income households with female and male providers spend at least as much on food per person as the typical

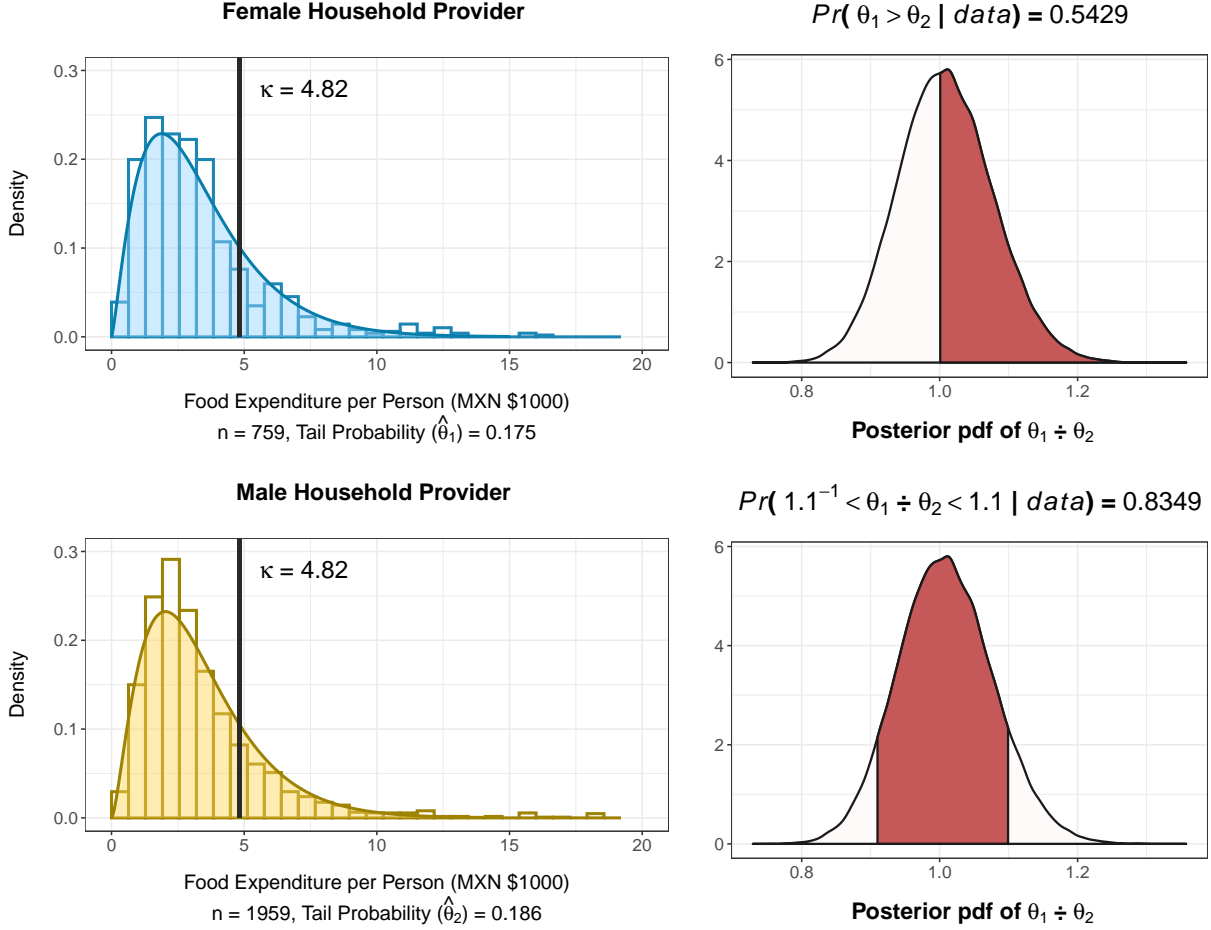


Figure 1: Group-specific summaries for quarterly food expenditure per person. Left: Food expenditure distributions. Right: Visualizations of the posterior probabilities.

upper income household. The observed proportions of households that spend at least \$4820 MXN on food per person are  $\hat{\theta}_1 = 0.175$  and  $\hat{\theta}_2 = 0.186$ . We assign uninformative  $\text{GAMMA}(2, 0.25)$  priors to both the shape  $\alpha_j$  and rate  $\beta_j$  parameters of the gamma model for group  $j = 1, 2$ . We let  $\boldsymbol{\eta}_j = (\alpha_j, \beta_j)$  for  $j = 1, 2$ . We obtain  $10^5$  posterior draws for  $\boldsymbol{\eta}_1$  and  $\boldsymbol{\eta}_2$  using Markov chain Monte Carlo (MCMC), which yields draws from the posterior of  $\theta_1/\theta_2$ . The gamma distributions characterized by the posterior means for  $\boldsymbol{\eta}_1$  and  $\boldsymbol{\eta}_2$  are superimposed on the histograms in Figure 1.

For concision, we demonstrate several example comparisons with posterior probabilities. Figure 1 illustrates that  $Pr(\theta_1/\theta_2 \in (1, \infty) \mid data) = 0.5429$ . We consider a conviction threshold of  $\gamma = 0.8$ . Because  $0.5429 \in (0.2, 0.8)$ , it is unclear whether households with female providers are at least as likely to spend  $\geq$  \$4820 MXN on food per person as those with male providers. We now suppose that a 10% relative increase or decrease in the gamma tail probability is not of practical importance. Figure 1 also indicates that  $Pr(\theta_1/\theta_2 \in (1.1^{-1}, 1.1) \mid data) = 0.8349$ . For  $\gamma = 0.8$ , this hypothesis test indicates that households with female providers are practically as likely to spend  $\geq$  \$4820 MXN on food per person as those with male

providers.

### 3 The Sampling Distribution of Posterior Probabilities

#### 3.1 Analytical Approximations to the Posterior

Traditional approaches to power curve approximation for posterior analyses require that we explore the sampling distribution of posterior probabilities for various sample sizes  $n$ . These approaches are slow for several reasons. First, in the absence of conjugate priors, we typically use computational methods to approximate the posterior for each generated sample. Second, we must simulate many samples from the prior predictive distribution of  $\mathbf{Y}^{(n)}$  to reliably estimate power for each value of  $n$  explored. Third, we may wastefully consider sample sizes for the study that are much too large or small when searching for a suitable sample size  $n$ . Our method for power curve approximation addresses these three sources of computational inefficiency. To address the first source of inefficiency, we leverage normal approximations to the posterior of  $\theta$  based on limiting results. In this subsection, we overview several analytical posterior approximation methods and conditions that must hold for these approximations to be suitable.

The first normal approximation to the posterior that we consider follows from the Bernstein-von Mises (BvM) theorem (van der Vaart, 1998). We now describe how our framework for power curve approximation satisfies the conditions for the BvM theorem. Our framework assumes that data  $y_{ij}$ ,  $i = 1, \dots, n_j$ ,  $j = 1, 2$  are to be collected independently, where the data generation process for group  $j$  is characterized by the model  $f(y; \boldsymbol{\eta}_{j,0})$  parameterized by  $\boldsymbol{\eta}_j \in \mathbb{R}^d$ . Here,  $f(\cdot)$  is the probability density or mass function selected for both groups of data, and  $\boldsymbol{\eta}_{1,0}$  and  $\boldsymbol{\eta}_{2,0}$  are (fixed) user-specified design values for the distributional parameter(s). These distributions are herein referred to as *design* distributions. The design values  $\boldsymbol{\eta}_{j,0}$  are different from the random variables  $\boldsymbol{\eta}_j$  that parameterize the model for groups  $j = 1, 2$  in Bayesian settings. When specifying the models  $f(y; \boldsymbol{\eta}_{j,0})$ , we also specify fixed values  $\theta_{j,0}$  for the random variables  $\theta_j$ ,  $j = 1, 2$ . These values are often specified implicitly as a function  $g(\cdot)$  of the parameters  $\boldsymbol{\eta}_{j,0}$ :  $\theta_{j,0} = g(\boldsymbol{\eta}_{j,0})$ . We require that  $g(\boldsymbol{\eta}_j)$  is differentiable at  $\boldsymbol{\eta}_j = \boldsymbol{\eta}_{j,0}$  for  $j = 1, 2$ . A fixed value for the univariate parameter  $\theta_0 = h(\theta_{1,0}, \theta_{2,0})$  is also specified, where  $h(\theta_1, \theta_2)$  is a differentiable function at  $\theta_1 = \theta_{1,0}$  and  $\theta_2 = \theta_{2,0}$ . These derivatives of  $g(\cdot)$  and  $h(\cdot)$  must be nonzero.

The four assumptions that must be satisfied to invoke the BvM theorem (van der Vaart, 1998) are detailed in Appendix A.1 of the supplement (Hagar and Stevens, 2023). The first three assumptions involve the models  $f(y; \boldsymbol{\eta}_{1,0})$  and  $f(y; \boldsymbol{\eta}_{2,0})$ ; they are weaker than the regularity conditions for the asymptotic normality of the maximum likelihood estimator (MLE) (Lehmann and Casella, 1998), which are listed in Appendix A.2 of the supplement. The final assumption for the BvM theorem regards prior specification for the random variables. For our purposes,  $\boldsymbol{\eta}_1$  and  $\boldsymbol{\eta}_2$  are the random variables for which we explicitly or implicitly assign prior distributions. We require that the prior distribution of  $\boldsymbol{\eta}_j$  be continuous in a neighbourhood of  $\boldsymbol{\eta}_{j,0}$  with

positive density at  $\boldsymbol{\eta}_{j,0}$  for  $j = 1, 2$ . This condition is important because it ensures that the posterior of  $\theta$  converges to a neighbourhood of  $\theta_0 = h(g(\boldsymbol{\eta}_{1,0}), g(\boldsymbol{\eta}_{2,0}))$ . This convergence is required for our method for power curve approximation introduced in Section 4.

Under the conditions for the BvM theorem, the posterior of  $\theta$  converges to the  $\mathcal{N}(\theta_0, \mathcal{I}(\theta_0)^{-1}/n)$  distribution in the limit of infinite data (van der Vaart, 1998), where  $\mathcal{I}(\theta_0)$  is the Fisher information for  $\theta$  evaluated at  $\theta_0$ . In practice,  $\theta_0$  is estimated from the to-be-observed data  $\mathbf{Y}^{(n)}$  using the MLE  $\hat{\theta}_n$  or the posterior mode  $\tilde{\theta}_n$ . In the limiting case, it does not matter which estimator for  $\theta$  is used because both  $\hat{\theta}_n$  and  $\tilde{\theta}_n$  converge in probability to  $\theta_0$  when the conditions for the BvM theorem are satisfied. We use the MLE instead of the posterior mode for reasons discussed in Section 3.2. We therefore consider the following normal distribution based on the BvM theorem as one option to approximate the posterior of  $\theta$ :

$$\mathcal{N}\left(h(g(\hat{\boldsymbol{\eta}}_{1,n}), g(\hat{\boldsymbol{\eta}}_{2,n})), \frac{1}{n} \sum_{j=1}^2 \left[ \frac{\partial h}{\partial \theta_j} \right]_{\theta_j=g(\hat{\boldsymbol{\eta}}_{j,n})}^2 \left[ \frac{\partial g^T}{\partial \boldsymbol{\eta}} \mathcal{I}(\boldsymbol{\eta})^{-1} \frac{\partial g}{\partial \boldsymbol{\eta}} \right]_{\boldsymbol{\eta}=\hat{\boldsymbol{\eta}}_{j,n}} \right). \quad (8)$$

To find  $\mathcal{I}(\boldsymbol{\eta})^{-1}$ , we find the limiting distributions for  $\sqrt{n}(\hat{\boldsymbol{\eta}}_{j,n} - \boldsymbol{\eta}_{j,0})$ ,  $j = 1, 2$ . The multivariate delta method prompts the distribution in (8) since  $\hat{\theta}_n = h(g(\hat{\boldsymbol{\eta}}_{1,n}), g(\hat{\boldsymbol{\eta}}_{2,n}))$  is a function of the MLEs  $\hat{\boldsymbol{\eta}}_{1,n}$  and  $\hat{\boldsymbol{\eta}}_{2,n}$ . We note that the variance in (8) is  $\mathcal{I}(\hat{\theta}_n)/n$ .

The approximation in (8) does not account for the priors, so we also consider the Laplace approximation to the posterior of  $\theta$ . This is useful when the sample size  $n$  is large enough to ensure the posterior is approximately normal but not large enough to guarantee the relevant priors have no substantial impact on the posterior mean and variance. For groups  $j = 1$  and  $2$ , the Laplace approximation is based on the Taylor series expansion of  $\log(p_j(\boldsymbol{\eta}_j | data))$  centered at the posterior mode  $\tilde{\boldsymbol{\eta}}_{j,n} = \arg \max_{\boldsymbol{\eta}_j} p_j(\boldsymbol{\eta}_j | data)$  (Gelman et al., 2013). The multivariate delta method prompts the following normal approximation to the posterior of  $\theta$  that accounts for the priors  $p_1(\boldsymbol{\eta}_1)$  and  $p_2(\boldsymbol{\eta}_2)$ :

$$\mathcal{N}\left(h(g(\tilde{\boldsymbol{\eta}}_{1,n}), g(\tilde{\boldsymbol{\eta}}_{2,n})), \sum_{j=1}^2 \left[ \frac{\partial h}{\partial \theta_j} \right]_{\theta_j=g(\tilde{\boldsymbol{\eta}}_{j,n})}^2 \left[ \frac{\partial g^T}{\partial \boldsymbol{\eta}} \mathcal{J}_j(\boldsymbol{\eta})^{-1} \frac{\partial g}{\partial \boldsymbol{\eta}} \right]_{\boldsymbol{\eta}=\tilde{\boldsymbol{\eta}}_{j,n}} \right), \quad (9)$$

$$\text{where } \mathcal{J}_j(\boldsymbol{\eta}) = -\frac{\partial^2}{\partial \boldsymbol{\eta}^2} \log(p_j(\boldsymbol{\eta} | data)).$$

We can quickly compute probabilities for the normal approximation to the posterior of  $\theta$  prompted by (8) or (9). When the sample size  $n$  is sufficiently large, these analytical approximation methods therefore mitigate the first source of inefficiency associated with computational power curve approximation. While it does not account for the priors, the approximation in (8) is useful because it prompts theoretical results about the limiting behaviour of the sampling distribution of posterior probabilities in Section 3.4. Moreover, the Laplace approximation in (9) is computationally burdensome and suboptimal in certain situations as explained in Section 3.3.

### 3.2 Dimension Reduction for Sampling Distribution Exploration

We next address the inefficiency with generating many samples from the design distributions to estimate the sampling distribution of posterior probabilities for each sample size  $n$  explored. To do so, we propose methods to reduce the simulation dimension when using normal approximations to the posterior that do not and do account for the priors in this subsection and Section 3.3, respectively. The methods presented in the remainder of this section allow us to greatly reduce the number of posteriors required to obtain precise power estimates in Section 4.

To generate samples of size  $n$  from each design distribution  $f(y; \boldsymbol{\eta}_{1,0})$  and  $f(y; \boldsymbol{\eta}_{2,0})$ , we typically require a pseudorandom sequence  $\mathbf{u}_1, \mathbf{u}_2, \dots, \mathbf{u}_m \in [0, 1]^{2n}$  with length  $m$ . This sequence is high dimensional unless the sample size  $n$  is rather small. However, the approximation in (8) does not directly use the observations from the generated sample  $\mathbf{y}^{(n)}$ . Instead,  $\mathbf{y}^{(n)}$  is used to compute maximum likelihood estimates  $\hat{\boldsymbol{\eta}}_{1,n}$  and  $\hat{\boldsymbol{\eta}}_{2,n}$ , which yield  $\hat{\theta}_n = h(g(\hat{\boldsymbol{\eta}}_{1,n}), g(\hat{\boldsymbol{\eta}}_{2,n}))$ . As such, we do not simulate data  $\mathbf{Y}^{(n)}$  from the prior predictive distribution for a given sample size  $n$ . We instead simulate from the approximate distributions for the MLEs of  $\boldsymbol{\eta}_1$  and  $\boldsymbol{\eta}_2$ .

For sufficiently large  $n$ , the MLEs  $\hat{\boldsymbol{\eta}}_{j,n}$  for groups  $j = 1, 2$  approximately and independently follow  $\mathcal{N}(\boldsymbol{\eta}_{j,0}, \mathcal{I}^{-1}(\boldsymbol{\eta}_{j,0})/n)$  distributions. The MLE – and not the posterior mode – is used with the approximation in (8) because we can easily simulate from its limiting distribution. Both  $\hat{\boldsymbol{\eta}}_{1,n}$  and  $\hat{\boldsymbol{\eta}}_{2,n}$  have dimension  $d$ , so their joint limiting distribution has dimension  $2d$ . When using pseudorandom number generation, we now require a sequence  $\mathbf{u}_1, \mathbf{u}_2, \dots, \mathbf{u}_m \in [0, 1]^{2d}$ . The dimension of the data  $\mathbf{Y}^{(n)}$  is typically such that  $d \ll n$ . Algorithm 1 details how we use a single point  $\mathbf{u} = (u_1, u_2, \dots, u_{2d}) \in [0, 1]^{2d}$  to obtain the posterior approximation based on the BvM theorem in (8), where  $\hat{\boldsymbol{\eta}}_{j,n}^{(k)}$  and  $\boldsymbol{\eta}_{j,0}^{(k)}$  denote the  $k^{\text{th}}$  component of these vectors.

---

**Algorithm 1** Low-Dimensional Posterior Approximation with the BvM Theorem

---

- 1: **procedure** APPROXBVM( $f(y; \boldsymbol{\eta}_{1,0}), f(y; \boldsymbol{\eta}_{2,0}), g(\cdot), h(\cdot), n, \mathbf{u}$ )
  - 2:   **for**  $j$  in  $[1, 2]$  **do**
  - 3:     **for**  $k$  in  $[1, d]$  **do**
  - 4:       Generate  $\hat{\boldsymbol{\eta}}_{j,n}(\mathbf{u})^{(k)}$  as the  $u_{(j-1)d+k}$ -quantile of the  $\mathcal{N}(\boldsymbol{\eta}_{j,0}^{(k)}, \mathcal{I}(\boldsymbol{\eta}_{j,0}^{(k)})^{-1}/n)$  CDF conditional on  $\hat{\boldsymbol{\eta}}_{j,n}(\mathbf{u})^{(0)}, \dots, \hat{\boldsymbol{\eta}}_{j,n}(\mathbf{u})^{(k-1)}$ .
  - 5:   Use  $\hat{\boldsymbol{\eta}}_{1,n}(\mathbf{u}), \hat{\boldsymbol{\eta}}_{2,n}(\mathbf{u})$ , and the partial derivatives of  $g(\cdot)$  and  $h(\cdot)$  to obtain (8).
- 

In practice, we may require fewer observations for the approximate distributions of the MLEs to be approximately normal if we consider some transformation of  $\boldsymbol{\eta}_j$ . For the gamma model, both parameters in  $\boldsymbol{\eta}_j = (\alpha_j, \beta_j)$  must be positive, but the  $\mathcal{N}(\boldsymbol{\eta}_{j,0}, \mathcal{I}^{-1}(\boldsymbol{\eta}_{j,0})/n)$  distribution could admit nonpositive values for small  $n$ . To obtain a sample of positive  $\hat{\boldsymbol{\eta}}_{1,n}$  and  $\hat{\boldsymbol{\eta}}_{2,n}$  values for any sample size  $n$  with the gamma model, we exponentiate a sample of approximately normal MLEs of  $\log(\boldsymbol{\eta}_1)$  and  $\log(\boldsymbol{\eta}_2)$ . For an arbitrary model, appropriate transformations could similarly be applied to any parameters in  $\boldsymbol{\eta}_j$  that do not have

support on  $\mathbb{R}$ . Similarly, the posterior of a monotonic transformation of  $\theta$  may need to be considered for the normal approximation in (8) to be suitable for moderate  $n$ . For instance, the posterior of  $\log(\theta_1) - \log(\theta_2)$  may better approximate a normal distribution than that of  $\theta_1/\theta_2$ . Rather than introduce new notation for these untransformed and transformed variables, we assume that  $\boldsymbol{\eta}_1$ ,  $\boldsymbol{\eta}_2$ , and  $\theta$  are specified to improve the quality of the relevant normal approximations in (8) and (9). Because priors are typically specified for  $\boldsymbol{\eta}_1$  and  $\boldsymbol{\eta}_2$  before making such transformations, relevant Jacobians must be considered when using normal approximations to the posterior that account for the prior distributions.

### 3.3 Dimension Reduction with Prior Information

The dimension reduction method proposed in Section 3.2 uses the posterior approximation in (8) that does not account for the prior distributions. The Laplace approximation to the posterior of  $\theta$  in (9) that accounts for the priors requires an observed sample  $\mathbf{y}^{(n)}$  – not just the maximum likelihood estimates  $\hat{\boldsymbol{\eta}}_{1,n}$  and  $\hat{\boldsymbol{\eta}}_{2,n}$ . In this subsection, we present two methods for low-dimensional posterior approximation that account for the priors. The first method is ideal when the design distributions belong to the exponential family (Lehmann and Casella, 1998), whereas the second method allows for more flexibility when specifying the models  $f(y; \boldsymbol{\eta}_{1,0})$  and  $f(y; \boldsymbol{\eta}_{2,0})$ .

When the design distributions belong to the exponential family, the relevant probability mass or density function takes the form

$$f(y; \boldsymbol{\eta}_j) = \exp \left[ \sum_{s=1}^d C_s(\boldsymbol{\eta}_j) T_s(y) - A(\boldsymbol{\eta}_j) + B(y) \right],$$

where  $A(\boldsymbol{\eta}_j)$ ,  $B(y)$ ,  $C_s(\boldsymbol{\eta}_j)$ , and  $T_s(y)$  are known functions for  $s = 1, \dots, d$ . For group  $j$ ,  $T_{j\ddagger}(\mathbf{y}^{(n)}) = (\sum_{i=1}^n T_1(y_{ij}), \dots, \sum_{i=1}^n T_d(y_{ij}))$  are called sufficient statistics that provide as much information about the parameter  $\boldsymbol{\eta}_j$  as the entire sample. The first derivative of the log-likelihood with respect to the  $k^{\text{th}}$  component of  $\boldsymbol{\eta}_j$  is then

$$\frac{\partial}{\partial \boldsymbol{\eta}_j^{(k)}} l(\boldsymbol{\eta}_j; \mathbf{y}^{(n)}) = n \frac{\partial}{\partial \boldsymbol{\eta}_j^{(k)}} A(\boldsymbol{\eta}_j) + \sum_{s=1}^d \frac{\partial}{\partial \boldsymbol{\eta}_j^{(k)}} C_s(\boldsymbol{\eta}_j) \sum_{i=1}^n T_s(y_{ij}). \quad (10)$$

At the maximum likelihood estimate  $\hat{\boldsymbol{\eta}}_{j,n}$  for an observed sample  $\mathbf{y}^{(n)}$ , all  $d$  partial derivatives in (10) equal 0. A  $d$ -parameter model in the exponential family has  $d$  nonredundant sufficient statistics, so all components of  $T_{j\ddagger}(\mathbf{y}^{(n)})$  can be recovered by substituting the maximum likelihood estimate  $\hat{\boldsymbol{\eta}}_{j,n}$  into the system of linear equations in (10). Algorithm 2 details how we use a single point  $\mathbf{u} \in [0, 1]^{2d}$  to obtain the posterior approximation in (9) based on Laplace’s method. For models  $f(y; \boldsymbol{\eta}_{1,0})$  and  $f(y; \boldsymbol{\eta}_{2,0})$  in exponential family, we emphasize that  $p_j(\boldsymbol{\eta}_j | \text{data}) = p_j(\boldsymbol{\eta}_j | T_{j\ddagger}(\mathbf{y}^{(n)}))$  for  $j = 1, 2$ .

However, Algorithm 2 may not provide a serviceable approach when the design distributions are not members of the exponential family. For instance, this method could not be applied if a Weibull model were chosen for the motivating example in Section 2 in lieu of the gamma distribution. When the shape parameter of the Weibull distribution is unknown, its minimal sufficient statistic consists of the entire sample:

---

**Algorithm 2** Low-Dimensional Posterior Approximation with Laplace's Method
 

---

- 1: **procedure** APPROXLAPLACE( $f(y; \boldsymbol{\eta}_{1,0}), f(y; \boldsymbol{\eta}_{2,0}), g(\cdot), h(\cdot), n, \mathbf{u}, p_1(\boldsymbol{\eta}_1), p_2(\boldsymbol{\eta}_2)$ )
  - 2:   Generate  $\hat{\boldsymbol{\eta}}_{1,n}(\mathbf{u})$  and  $\hat{\boldsymbol{\eta}}_{2,n}(\mathbf{u})$  using Lines 2 to 4 of Algorithm 1.
  - 3:   **for**  $j$  in  $[1, 2]$  **do**
  - 4:     Solve the system of equations in (10) with  $\boldsymbol{\eta}_j = \hat{\boldsymbol{\eta}}_{j,n}(\mathbf{u})$  to obtain  $T_{j\dagger}(\mathbf{y}^{(n)})$ .
  - 5:     Use  $T_{j\dagger}(\mathbf{y}^{(n)})$  to obtain the posterior mode  $\tilde{\boldsymbol{\eta}}_{j,n}$  via optimization.
  - 6:   Use  $\tilde{\boldsymbol{\eta}}_{1,n}(\mathbf{u}), \tilde{\boldsymbol{\eta}}_{2,n}(\mathbf{u}), T_{1\dagger}(\mathbf{y}^{(n)})$ , and  $T_{2\dagger}(\mathbf{y}^{(n)})$  along with the partial derivatives of  $g(\cdot)$  and  $h(\cdot)$  to obtain (9).
- 

$y_{ij}$ ,  $i = 1, \dots, n$  for  $j = 1, 2$ . We therefore develop a hybrid approach to analytical posterior approximation that accounts for the priors when low-dimensional sufficient statistics cannot be recovered from the maximum likelihood estimates  $\hat{\boldsymbol{\eta}}_{1,n}$  and  $\hat{\boldsymbol{\eta}}_{2,n}$ .

This hybrid approach leverages the following result, which holds true when  $\boldsymbol{\eta}_j \approx \hat{\boldsymbol{\eta}}_{j,n}$  for sufficiently large  $n$ :

$$\log(p_j(\boldsymbol{\eta}_j | \mathbf{y}^{(n)})) \approx l(\hat{\boldsymbol{\eta}}_{j,n}; \mathbf{y}^{(n)}) - \frac{n}{2}(\boldsymbol{\eta}_j - \hat{\boldsymbol{\eta}}_{j,n})^T \mathcal{I}(\hat{\boldsymbol{\eta}}_{j,n})(\boldsymbol{\eta}_j - \hat{\boldsymbol{\eta}}_{j,n}) + \log(p_j(\boldsymbol{\eta}_j)). \quad (11)$$

This result follows from the second-order Taylor approximation to the log-posterior of  $\boldsymbol{\eta}_j$  around  $\hat{\boldsymbol{\eta}}_{j,n}$ , where the observed information is replaced with the (expected) Fisher information. The approximation to the log-likelihood function does not have a first-order term because the score function is 0 at  $\hat{\boldsymbol{\eta}}_{j,n}$ . We note that although the first term on the right side of (11) depends on the data  $\mathbf{y}^{(n)}$ , it is a constant. An approximation to the posterior mode is the value that maximizes the right side of (11):  $\boldsymbol{\eta}_{j,n}^*$ . We consider the following normal approximation to the posterior of  $\theta$ :

$$\mathcal{N} \left( h(g(\boldsymbol{\eta}_{1,n}^*), g(\boldsymbol{\eta}_{2,n}^*)), \sum_{j=1}^2 \left[ \frac{\partial h}{\partial \theta_j} \right]_{\theta_j = g(\boldsymbol{\eta}_{j,n}^*)}^2 \left[ \frac{\partial g^T}{\partial \boldsymbol{\eta}} \mathcal{J}_j^*(\boldsymbol{\eta})^{-1} \frac{\partial g}{\partial \boldsymbol{\eta}} \right]_{\boldsymbol{\eta} = \boldsymbol{\eta}_{j,n}^*} \right), \quad (12)$$

$$\text{where } \mathcal{J}_j^*(\boldsymbol{\eta}) = n\mathcal{I}(\boldsymbol{\eta}) - \frac{\partial^2}{\partial \boldsymbol{\eta}^2} \log(p_j(\boldsymbol{\eta})).$$

The observed information is again replaced with the Fisher information in  $\mathcal{J}_j^*(\boldsymbol{\eta})$  of (12) since we do not generate samples  $\mathbf{y}^{(n)}$ . Algorithm 3 details how we can obtain the posterior approximation in (12) using a single point  $\mathbf{u} \in [0, 1]^{2d}$ .

---

**Algorithm 3** Low-Dimensional Posterior Approximation with Hybrid Method
 

---

- 1: **procedure** APPROXHYBRID( $f(y; \boldsymbol{\eta}_{1,0}), f(y; \boldsymbol{\eta}_{2,0}), g(\cdot), h(\cdot), n, \mathbf{u}, p_1(\boldsymbol{\eta}_1), p_2(\boldsymbol{\eta}_2)$ )
  - 2:   Generate  $\hat{\boldsymbol{\eta}}_{1,n}(\mathbf{u})$  and  $\hat{\boldsymbol{\eta}}_{2,n}(\mathbf{u})$  using Lines 2 to 4 of Algorithm 1.
  - 3:   **for**  $j$  in  $[1, 2]$  **do**
  - 4:     Obtain  $\boldsymbol{\eta}_{j,n}^*$  as  $\arg \max_{\boldsymbol{\eta}_j}$  of the right side of (11) when  $\boldsymbol{\eta}_{j,n} = \hat{\boldsymbol{\eta}}_{j,n}(\mathbf{u})$ .
  - 5:   Use  $\boldsymbol{\eta}_{1,n}^*, \boldsymbol{\eta}_{2,n}^*$ , and the partial derivatives of  $g(\cdot)$  and  $h(\cdot)$  to obtain (12).
-

### 3.4 Theoretical Properties of the Power Estimates

Now that we have developed three algorithms to reduce the simulation dimension in a variety of settings, we consider the theoretical properties of the resulting power estimates. We introduce general notation to define power estimates for the simulation method  $\zeta$ , where  $\zeta$  is Algorithm 1, 2, or 3. We let  $\mathcal{N}(\underline{\theta}_r^{(n)}, \underline{\tau}_r^{(n)})$  denote the relevant normal approximation to the posterior of  $\theta$  corresponding to the point  $\mathbf{u}_r \in [0, 1]^{2d}$  and sample size  $n$  for  $r = 1, \dots, m$ . This approximation is respectively (8) for Algorithm 1, (9) for Algorithm 2, and (12) for Algorithm 3. We incorporate the sample size  $n$  into this notation because the mean  $\underline{\theta}_r^{(n)}$  depends on the sample size of the joint limiting distribution for  $\hat{\boldsymbol{\eta}}_{1,n}$  and  $\hat{\boldsymbol{\eta}}_{2,n}$ . The variance  $\underline{\tau}_r^{(n)}$  is also an explicit function of  $n$  in (8) and (12) and an implicit function of the sample size in (9).

The estimate for the posterior probability  $Pr(\theta < \delta \mid \text{data})$  is then

$$p_{n, \mathbf{u}_r, \zeta}^\delta = \Phi \left( \frac{\delta - \underline{\theta}_r^{(n)}}{\sqrt{\underline{\tau}_r^{(n)}}} \right), \quad (13)$$

where  $\Phi(\cdot)$  is the cumulative distribution function (CDF) of the standard normal distribution. The estimates from (13) can be used to determine whether the criterion inside the indicator function from (4) or (7) is satisfied for a particular posterior approximation  $\mathcal{N}(\underline{\theta}_r^{(n)}, \underline{\tau}_r^{(n)})$ . For a given sample size  $n$ , the proportion of the  $m$  approximate posteriors corresponding to  $\mathbf{u}_1, \dots, \mathbf{u}_m$  for which the relevant criterion is satisfied estimates power. Because the limiting posterior of  $\theta$  is normal when the conditions for the BvM theorem hold, power for hypothesis testing with HDIs defined in (6) should be approximated by power defined in (7) for sufficiently large  $n$ .

No matter which of our three algorithms are used, the accuracy of these power estimates depends on the quality of the approximation to the sampling distribution of posterior probabilities. If data  $\mathbf{Y}^{(n)}$  are generated from the design distributions and the assumptions for the BvM theorem hold true, the normal approximations to the posterior of  $\theta$  given in (8) and (9) are well established. Theorem 1 first compares the sampling distributions of posterior probabilities induced by those normal approximations with data  $\mathbf{Y}^{(n)}$  to the sampling distribution prompted by Algorithm 1 with pseudorandom sequences as  $n \rightarrow \infty$ .

**Theorem 1.** *Let  $f(y; \boldsymbol{\eta}_{1,0})$  and  $f(y; \boldsymbol{\eta}_{2,0})$  satisfy the regularity conditions from Appendix A.2. Let the prior  $p_j(\boldsymbol{\eta}_j)$  be continuous in a neighbourhood of  $\boldsymbol{\eta}_{j,0}$  with positive density at  $\boldsymbol{\eta}_{j,0}$  for  $j = 1, 2$ . Let  $g(\boldsymbol{\eta})$  and  $h(\theta_1, \theta_2)$  be respectively differentiable at  $\boldsymbol{\eta}_{j,0}$  and  $\theta_{j,0} = g(\boldsymbol{\eta}_{j,0})$  for  $j = 1, 2$  with nonzero derivatives. Let  $\mathbf{U} \stackrel{i.i.d.}{\sim} \mathcal{U}([0, 1]^{2d})$  and  $\mathbf{Y}^{(n)}$  be generated independently from  $f(y; \boldsymbol{\eta}_{1,0})$  and  $f(y; \boldsymbol{\eta}_{2,0})$ . Let  $\mathcal{P}_{n, \Pi, \zeta}^\delta$  denote the sampling distribution of posterior probabilities for  $Pr(\theta < \delta \mid \text{data})$  given sample size  $n$  produced using input  $\Pi$  with method  $\zeta$ . Then,*

$$(a) \mathcal{P}_{n, \mathbf{Y}^{(n)}, (8)}^\delta \xrightarrow{d} \mathcal{P}_{n, \mathbf{U}, Alg. 1}^\delta$$

$$(b) \mathcal{P}_{n, \mathbf{Y}^{(n)}, (9)}^\delta \xrightarrow{d} \mathcal{P}_{n, \mathbf{U}, Alg. 1}^\delta$$

The proof of Theorem 1 is given in Appendix A.3 of the supplement. While the approximations in (9) and (12) should better account for the prior distributions for moderate sample sizes  $n$ , they do not differ from the approximation in (8) in the limit of infinite data. Likewise,  $\mathcal{P}_{n,\mathcal{U},\text{Alg.2}}^\delta$  and  $\mathcal{P}_{n,\mathcal{U},\text{Alg.3}}^\delta$  will converge in distribution to  $\mathcal{P}_{n,\mathcal{U},\text{Alg.1}}^\delta$  as  $n \rightarrow \infty$  under the conditions for Theorem 1. This result is straightforward because  $\tilde{\boldsymbol{\eta}}_{j,n} - \hat{\boldsymbol{\eta}}_{j,n}$  and  $\boldsymbol{\eta}_{j,n}^* - \hat{\boldsymbol{\eta}}_{j,n}$  converge in probability to 0, and  $\mathcal{J}_j(\tilde{\boldsymbol{\eta}}_{j,n})/n$  and  $\mathcal{J}_j^*(\boldsymbol{\eta}_{j,n}^*)/n$  converge in probability to  $\mathcal{I}(\boldsymbol{\eta}_{j,0})$  given results from Appendix A.3. These results prompt Corollary 1, which follows from Theorem 1.

**Corollary 1.** *Let  $p_{n,\mathbf{u}_r,\zeta}^\delta$  from (13) be the estimate for  $\Pr(\theta < \delta \mid \text{data})$  corresponding to sample size  $n$ , method  $\zeta$ , and point  $\mathbf{u}_r \in [0, 1]^{2d}$ . Under the conditions for Theorem 1, power in (4) and (7) are consistently estimated by*

$$\frac{1}{m} \sum_{r=1}^m \mathbb{I}(p_{n,\mathbf{u}_r,\zeta}^{\delta_U} - p_{n,\mathbf{u}_r,\zeta}^{\delta_L} \geq \gamma) \quad \text{and} \quad \frac{1}{m} \sum_{r=1}^m \mathbb{I}(p_{n,\mathbf{u}_r,\zeta}^{\delta_L} < \alpha/2 \cap 1 - p_{n,\mathbf{u}_r,\zeta}^{\delta_U} < \alpha/2),$$

respectively, when  $\zeta$  is Algorithm 1, 2, or 3 and  $\mathbf{U}_r \stackrel{i.i.d.}{\sim} \mathcal{U}([0, 1]^{2d})$  for  $r = 1, \dots, m$  as  $n \rightarrow \infty$ .

Corollary 1 ensures that our three algorithms give rise to consistent power estimates as  $n \rightarrow \infty$ ; however, it does not guarantee that these estimators are unbiased for finite  $n$ . When the assumptions for Theorem 1 are satisfied, our power estimates are suitable for sufficiently large  $n$ . To optimize the performance of these design methods for moderate  $n$ , one should consider transformations of  $\theta$  or certain components in  $\boldsymbol{\eta}_1$  and  $\boldsymbol{\eta}_2$  to improve the normal approximations to the relevant posterior and MLE distributions.

## 4 A Fast Method for Power Curve Approximation

The methods in the previous section have not directly allowed us to reduce the number of posteriors required to precisely estimate power at a given sample size  $n$ . We have also not yet addressed how to efficiently explore the sample size space. In this section, we propose an approach that uses the methods from Section 3 to reduce the number of posteriors required for power estimation and sample size exploration. That approach detailed in Algorithm 4 is the main contribution of this paper.

### 4.1 Power Estimates with Fewer Posteriors

This subsection details how we use low-discrepancy sequences to reduce the number of posteriors required to precisely estimate power at each sample size  $n$  explored. Unlike pseudorandom sequences, low-discrepancy sequences induce negative dependence between the points  $\mathbf{U}_1, \dots, \mathbf{U}_m$ . We use a particular class of low-discrepancy sequences called Sobol' sequences (Sobol', 1967). Sobol' sequences are created deterministically based on integer expansion in base 2, and they are regularly incorporated into quasi-Monte Carlo methods (Lemieux, 2009). Randomized Sobol' sequences yield estimators with better consistency properties than those created using purely deterministic sequences, and this randomization can be carried out via a digital

shift (Lemieux, 2009). We generate and randomize Sobol’ sequences in R using the `qrng` package (Hofert and Lemieux, 2020).

When using randomized Sobol’ sequences, each point in the sequence is such that  $\mathbf{U}_r \sim U([0, 1]^{2d})$  for  $r = 1, \dots, m$ . It follows that randomized Sobol’ sequences can be used similarly to pseudorandom sequences in Monte Carlo simulation to prompt unbiased estimators:

$$\mathbb{E} \left( \frac{1}{m} \sum_{r=1}^m \Psi(\mathbf{U}_r) \right) = \int_{[0,1]^{2d}} \Psi(\mathbf{u}) d\mathbf{u}, \quad (14)$$

for some function  $\Psi(\cdot)$ . Corollary 2 follows from (14), where either indicator function in Corollary 1 is the relevant function  $\Psi(\cdot)$ .

**Corollary 2.** *Under the conditions for Theorem 1, using a randomized low-discrepancy sequence  $\mathbf{U}_1, \dots, \mathbf{U}_m$  in lieu of a sequence  $\mathbf{U}_r \stackrel{i.i.d.}{\sim} \mathcal{U}([0, 1]^{2d})$  for  $r = 1, \dots, m$  does not impact the consistency of the power estimates from Corollary 1 as  $n \rightarrow \infty$ .*

Due to the negative dependence between the points, the variance of the estimator in (14) is typically reduced by using low-discrepancy sequences. We have that

$$\text{Var} \left( \frac{1}{m} \sum_{r=1}^m \Psi(\mathbf{U}_r) \right) = \frac{\text{Var}(\Psi(\mathbf{U}_r))}{m} + \frac{2}{m^2} \sum_{r=1}^m \sum_{t=r+1}^m \text{Cov}(\Psi(\mathbf{U}_r), \Psi(\mathbf{U}_t)), \quad (15)$$

where the the first term on the right side of (15) is the variance of the corresponding estimator based on pseudorandom sequences of independently generated points. While underutilized in experimental design, low-discrepancy sequences give rise to effective variance reduction methods when the dimension of the simulation is moderate. However, high-dimensional low-discrepancy sequences may have poor low-dimensional projections, which can lead to a deterioration in performance. This is why we proposed the low-dimensional posterior approximation methods in Section 3. We can readily find a suitable Sobol’ sequence of dimension  $2d$ , but it may be challenging to find an appropriate sequence of dimension  $2n$  when the sample size is large. By (15), randomized Sobol’ sequences reduce the number of posteriors for  $\theta$  that we must approximate to obtain precise, consistent power estimates. This result addresses the second source of computational inefficiency associated with traditional power curve approximation.

## 4.2 Efficient Exploration of the Sample Size Space

For a given sample size  $n$ , we *could* obtain power estimates using the formulas in Corollary 1 with randomized Sobol’ sequences. Sample size determination could be conducted by repeating this process for various values of  $n$  until a suitable sample size is found. However, such a process would still waste computational resources exploring unsuitable sample sizes to obtain an appropriate one. We note that the  $(\theta_1, \theta_2)$ -space such that  $\theta = h(\theta_1, \theta_2) \in (\delta_L, \delta_U)$  is convex when  $\theta = \theta_1 - \theta_2$  or  $\theta = \theta_1/\theta_2$ . If we appeal to this convexity, we argue that consistent power estimates for a given sample size  $n$  can often be obtained with only a subset of the

points  $\mathbf{u}_r \in [0, 1]^{2d}$ ,  $r = 1, \dots, m$ . By using only a subset of points to explore most sample sizes, we address the final source of computational inefficiency associated with traditional power curve approximation.

In each of our algorithms, the approximately normal posterior  $\mathcal{N}(\underline{\theta}_r^{(n)}, \underline{\tau}_r^{(n)})$  and corresponding posterior probabilities  $p_{n, \mathbf{u}_r, \zeta}^\delta$  depend on the design distributions, the sample size  $n$ , and the Sobol' sequence point  $\mathbf{u}_r$ ,  $r = 1, \dots, m$ . We have previously fixed the sample size  $n$  and allowed the point  $\mathbf{u}_r \in [0, 1]^{2d}$  to vary when estimating power. We now fix the point  $\mathbf{u}_r$  and let the sample size  $n$  vary. When the point  $\mathbf{u}_r$  and design distributions are fixed,  $p_{n, \mathbf{u}_r, \zeta}^\delta$  is a deterministic function of  $n$ . Lemma 1 motivates our approach to circumventing the need to consider all points  $\mathbf{u}_r \in [0, 1]^{2d}$  for each sample size  $n$  explored.

**Lemma 1.** *Let the conditions for Theorem 1 be satisfied. For a given point  $\mathbf{u}_r = (u_1, \dots, u_{2d}) \in [0, 1]^{2d}$ , we have that Algorithms 1, 2, and 3 prompt*

$$(a) \hat{\boldsymbol{\eta}}_{1,n}(\mathbf{u}_r)^{(k)} = \boldsymbol{\eta}_{1,0}^{(k)} + \frac{\omega_k(u_1, \dots, u_k)}{\sqrt{n}} \text{ and } \hat{\boldsymbol{\eta}}_{2,n}(\mathbf{u}_r)^{(k)} = \boldsymbol{\eta}_{2,0}^{(k)} + \frac{\omega_{d+k}(u_{d+1}, \dots, u_{d+k})}{\sqrt{n}} \text{ for } k = 1, \dots, d, \text{ where } \omega_k(\cdot) \text{ and } \omega_{d+k}(\cdot) \text{ are functions that do not depend on } n.$$

$$(b) h(g(\hat{\boldsymbol{\eta}}_{1,n}(\mathbf{u}_r)), g(\hat{\boldsymbol{\eta}}_{2,n}(\mathbf{u}_r))) \approx h(g(\boldsymbol{\eta}_{1,0}), g(\boldsymbol{\eta}_{2,0})) + \frac{\omega_{\dagger}(u_1, \dots, u_{2d})}{\sqrt{n}} \text{ for sufficiently large } n, \text{ where } \omega_{\dagger}(\cdot) \text{ is a function that does not depend on } n.$$

$$(c) p_{n, \mathbf{u}_r, \zeta}^\delta \approx \Phi(a(\delta, \theta_0)\sqrt{n} + b(\mathbf{u}_r)) \text{ for sufficiently large } n, \text{ where } \theta_0 \text{ is the design value for } \theta \text{ and } a(\cdot) \text{ and } b(\cdot) \text{ are functions that do not depend on } n.$$

$$(d) \text{ When } \theta_0 \in (\delta_L, \delta_U), p_{n, \mathbf{u}_r, \zeta}^{\delta_U} - p_{n, \mathbf{u}_r, \zeta}^{\delta_L} \text{ is a increasing function of } n \text{ for sufficiently large sample sizes.}$$

We prove Lemma 1 in Appendix B of the supplement and now consider its implications when  $\theta_0 \in (\delta_L, \delta_U)$  for a given point  $\mathbf{u}_r$ . If  $p_{n_A, \mathbf{u}_r, \zeta}^{\delta_U} - p_{n_A, \mathbf{u}_r, \zeta}^{\delta_L} \geq \gamma$ , then  $p_{n_B, \mathbf{u}_r, \zeta}^{\delta_U} - p_{n_B, \mathbf{u}_r, \zeta}^{\delta_L} \geq \gamma$  for sufficiently large  $n_A < n_B$ . The  $(\theta_1, \theta_2)$ -space such that  $\theta = h(\theta_1, \theta_2) \in (\delta_L, \delta_U)$  is convex, which limits the potential for decreasing behaviour of  $p_{n, \mathbf{u}_r, \zeta}^{\delta_U} - p_{n, \mathbf{u}_r, \zeta}^{\delta_L}$  as a function of  $n$  for small and moderate sample sizes. In light of this, our method to approximate the power curve generates a single Sobol' sequence of length  $m$ . For hypothesis tests with posterior probabilities, we use root finding algorithms (Brent, 1973) to find the value for  $n$  such that  $p_{n, \mathbf{u}_r, \zeta}^{\delta_U} - p_{n, \mathbf{u}_r, \zeta}^{\delta_L} - \gamma = 0$  for  $r = 1, \dots, m$ . The empirical CDF of these  $m$  sample sizes approximates the power curve. As demonstrated in Section 4.3, this root-finding approach facilitates targeted sampling from  $[0, 1]^{2d}$  based on the sample size  $n$ . Since the posterior probabilities in Corollary 1 are functions of  $\mathbf{u}_r \in [0, 1]^{2d}$ , this approach also gives rise to targeted sampling from the approximate sampling distribution of posterior probabilities.

### 4.3 Power Curve Approximation with Targeted Sampling

Algorithm 4 formally describes our fast method for power curve approximation with analyses facilitated via posterior probabilities and Bayes factors. We later discuss the necessary modifications for analyses with credible intervals. To implement this approach, we must choose a parametric statistical model  $f(y; \boldsymbol{\eta})$ ,

functions  $g(\cdot)$  and  $h(\cdot)$ , priors  $p_1(\boldsymbol{\eta}_1)$  and  $p_2(\boldsymbol{\eta}_2)$ , and design values  $\boldsymbol{\eta}_{1,0}$  and  $\boldsymbol{\eta}_{2,0}$ . We recommend using visualization techniques to choose the design values, and the literature on prior elicitation could be of use when specifying the design distributions (Chaloner, 1996; Garthwaite et al., 2005; Johnson et al., 2010). We must also select an interval  $(\delta_L, \delta_U)$ , a conviction threshold  $\gamma$ , a target power  $\Gamma$ , a method  $\zeta$  consisting of one of the three algorithms proposed in Section 3, and the length of the Sobol' sequence  $m$ . We use  $m = 1024$  to balance the computational efficiency and precision of the approximation to the power curve.

---

**Algorithm 4** Procedure for Power Curve Approximation with Posterior Probabilities

---

```

1: procedure POWERCURVE( $f(y; \boldsymbol{\eta}_{1,0}), f(y; \boldsymbol{\eta}_{2,0}), g(\cdot), h(\cdot), p_1(\boldsymbol{\eta}_1), p_2(\boldsymbol{\eta}_2), (\delta_L, \delta_U), \gamma, \Gamma, \zeta, m$ )
2:   Let  $n_0$  equate the left side of (4) to  $\Gamma$  when  $p(\theta \mid \text{data}) \approx \mathcal{N}(\hat{\theta}_n, \mathcal{I}(\theta_0)^{-1}/n)$ 
3:   sampSobol  $\leftarrow$  NULL
4:   for  $r$  in  $[1, m]$  do
5:     Generate Sobol' sequence point  $\mathbf{u}_r$ 
6:     Let sampSobol[ $r$ ] solve  $p_{n, \mathbf{u}_r, \zeta}^{\delta_U} - p_{n, \mathbf{u}_r, \zeta}^{\delta_L} - \gamma = 0$  in terms of  $n$ , initializing the root-finding algorithm at  $\lceil n_0 \rceil$ 
7:   powerCurve  $\leftarrow$  empirical CDF of sampSobol
8:   Let  $n_*$  be the  $\Gamma$ -quantile of sampSobol
9:   for  $r$  in  $[1, m]$  do
10:    if sampSobol[ $r$ ]  $\leq n_*$  then
11:      if  $p_{n_*, \mathbf{u}_r, \zeta}^{\delta_U} - p_{n_*, \mathbf{u}_r, \zeta}^{\delta_L} - \gamma < 0$  then
12:        Repeat Line 6, initializing the root-finding algorithm at  $n_*$ 
13:      else
14:        if  $p_{n_*, \mathbf{u}_r, \zeta}^{\delta_U} - p_{n_*, \mathbf{u}_r, \zeta}^{\delta_L} - \gamma \geq 0$  then
15:          Repeat Line 6, initializing the root-finding algorithm at  $n_*$ 
16:   powerCurveFinal  $\leftarrow$  empirical CDF of sampSobol
17:   Let  $n^*$  be the  $\Gamma$ -quantile of sampSobol
18:   return powerCurveFinal,  $\lceil n^* \rceil$  as recommended sample size

```

---

Line 3 of Algorithm 4 uses the normal approximation in (8) with known variance to obtain a starting point  $n_0$  for the root-finding algorithm. We can obtain this starting point in a fraction of a second, and it should be close to the final sample size recommendation if uninformative priors are used. Since the root-finding algorithm is initialized at  $\lceil n_0 \rceil$  for all points  $\mathbf{u}_r$ ,  $r = 1, \dots, m$ , the entire sampling distribution of posterior probabilities is explored for that sample size. In Lines 4 to 6, the root-finding algorithm then facilitates targeted sampling from the approximate distribution of posterior probabilities for all other sample sizes considered. We complete the power curve approximation procedure by exploring the entire sampling distribution of posterior probabilities at the sample size  $n_*$  in Lines 9 to 15. If the statements in Lines 11 or 14 are true, this implies that  $p_{n, \mathbf{u}_r, \zeta}^{\delta_U} - p_{n, \mathbf{u}_r, \zeta}^{\delta_L} = \gamma$  for at least two distinct sample sizes  $n$ . For these points  $\mathbf{u}_r$ , we can reinitialize the root-finding algorithm at  $n_*$  to obtain a solution for each point that will make the power curve consistent at  $n_*$ . This consistency is a direct consequence of Corollary 2.

In Section 5, we conduct numerical studies to demonstrate the suitability of the power curves obtained by Algorithm 4 in various settings. These numerical results show that the if statements in Lines 11 and 14 are very rarely true for any point  $\mathbf{u}_r \in [0, 1]^{2d}$  when sample sizes are large enough for the BvM theorem to

hold. In those situations,  $n_* = n^*$  and both the power estimate at  $n^*$  and the sample size recommendation  $\lceil n^* \rceil$  are consistent. It is incredibly unlikely that  $n_*$  and  $n^*$  would differ substantially, but Lines 9 to 15 of Algorithm 4 could be repeated in that event, where the root-finding algorithm is initialized at  $n^*$  instead of  $n_*$ . These consistent sample size recommendations are not guaranteed to be unbiased since the normal approximation to the relevant posterior and MLE distributions may introduce noticeable bias for finite  $n$ . Even though the power curves from Algorithm 4 are consistent near the target power  $\Gamma$ , their global consistency at all sample sizes  $n$  is not guaranteed because part (b) of Lemma 1 and the BvM theorem are large-sample results. Nevertheless, our numerical studies in Section 5 highlight good global estimation of the power curve, particularly when the posterior approximation method  $\zeta$  accounts for the priors.

The computational efficiency of this power curve approximation method justifies its use when the conditions for the BvM theorem are satisfied. The root-finding algorithm from Lines 4 to 6 of Algorithm 4 approximates posteriors corresponding to  $O(\log_2 B)$  points from  $[0, 1]^{2d}$ , where  $B$  is the maximum sample size considered for the power curve. We would require  $O(B)$  such points to explore a similar range of sample sizes using power estimates obtained via Corollary 1 with randomized Sobol' sequences. When  $B \geq 59$ , our approach prompts at least an order of magnitude reduction in the number of posterior approximations because  $O(\log_2 B) < O(B)/10$ . Moreover, using randomized Sobol' sequences in lieu of pseudorandom sequences has generally allowed us to estimate power curves with similar precision using an order of magnitude fewer points from  $[0, 1]^{2d}$ . We visualize the results from this paragraph using a simpler example than the four-dimensional one with gamma tail probabilities in Appendix C of the supplement.

We discuss how to generalize Algorithm 4 for analyses with credible intervals below. If one of  $\delta_L$  or  $\delta_U$  is not finite, Algorithm 4 can be used without modification where  $\gamma = 1 - \alpha$ . Otherwise, the initial value for the root-finding algorithm  $n_0$  found in Line 3 is based on (7) instead of (4). In Line 6, `sampSobol[r]` is modified to be the maximum of the two solutions for  $p_{n, \mathbf{u}_r, \zeta}^{\delta_L} - (1 - \alpha/2) = 0$  and  $1 - p_{n, \mathbf{u}_r, \zeta}^{\delta_U} - (1 - \alpha/2) = 0$ . We lastly modify how the sampling distribution of posterior probabilities at the sample size  $n_*$  is explored. To do so, we confirm that both  $p_{n_*, \mathbf{u}_r, \zeta}^{\delta_L} - (1 - \alpha/2)$  and  $1 - p_{n_*, \mathbf{u}_r, \zeta}^{\delta_U} - (1 - \alpha/2)$  are not less than or at least 0 in Lines 11 and 14, respectively. Effectively, power curve approximation with equal-tailed credible intervals requires us to consider two hypothesis tests with posterior probabilities and intervals  $(\delta_L, \infty)$  and  $(-\infty, \delta_U)$ .

## 5 Numerical Studies

### 5.1 Power Curve Approximation with the Gamma Distribution

We now compare the performance of our power curve approximation procedure across several scenarios. For each scenario, we specify design values for the gamma tail probability example from Section 2. Because the ENIGH survey is conducted biennially, we choose design values for both gamma distributions using data from the ENIGH 2018 survey (INEGI, 2019). We repeat the process detailed in Section 2 to create a

similar data set of 2018 quarterly food expenditure per person. We adjust each expenditure to account for inflation, compounding 2% annually, between 2018 and 2020. We find the posterior means for the gamma shape and rate parameters to be  $\bar{\alpha}_1 = 2.11$  and  $\bar{\beta}_1 = 0.69$  for the female provider group and  $\bar{\alpha}_2 = 2.43$  and  $\bar{\beta}_2 = 0.79$  for the male provider group. These posterior means comprise the design values  $\boldsymbol{\eta}_{1,0}$  and  $\boldsymbol{\eta}_{2,0}$ . After accounting for inflation, the 2018 estimate for the median quarterly food expenditure per person in upper income households is 4.29 (MXN \$1000). For the purposes of sample size determination, we use  $\kappa_0 = 4.29$  as the threshold for the gamma tail probabilities.

The scenarios we consider are based on two sets of prior distributions. For the first set, we specify uninformative GAMMA(2, 0.25) priors for the gamma parameters  $\alpha_j$  and  $\beta_j$  for group  $j = 1, 2$ . To choose the second set of priors, we reconsider the approximately gamma distributed posteriors used to obtain design values for  $\alpha_1, \beta_1, \alpha_2,$  and  $\beta_2$ . To incorporate prior information, we consider gamma distributions that have the same modes with variances that are larger by a factor of 10. In comparison to the GAMMA(2, 0.25) prior, these distributions are quite informative. These distributions – which we use as the set of informative priors – are GAMMA(34.23, 15.85) for  $\alpha_1$ , GAMMA(27.20, 38.15) for  $\beta_1$ , GAMMA(105.31, 42.96) for  $\alpha_2$ , and GAMMA(85.49, 106.58) for  $\beta_2$ .

For each prior specification, we first consider the quality of power curve estimation for analyses with posterior probabilities. We consider three  $((\delta_L, \delta_U), \gamma, \Gamma)$  combinations:  $\{a, b, c\} = \{((1.25^{-1}, 1.25), 0.5, 0.6), ((1.3^{-1}, \infty), 0.9, 0.7), ((1.15^{-1}, 1.15), 0.8, 0.8)\}$ . The first combination explores moderate sample sizes. The second combination considers a one-sided noninferiority hypothesis for  $\theta_1$ . We do not use the interval  $(\delta_L, \delta_U) = (1, \infty)$  corresponding to the superiority of  $\theta_1$  from Section 2. The design values are such that  $\theta_{1,0} = 0.174 \approx \theta_{2,0} = 0.168$ , so we would require an impractically large sample to support the hypothesis  $H_0 : \theta_1/\theta_2 \in (1, \infty)$ . The third combination explores larger sample sizes. This gives rise to six settings, each consisting of a prior specification (Setting 1 = uninformative, Setting 2 = informative) and  $((\delta_L, \delta_U), \gamma, \Gamma)$  combination.

For each setting, we generated 100 power curves using Algorithm 4 with  $\zeta = \{\text{Alg. 1, Alg. 2}\}$ . We do not consider Algorithm 3 for this example because the gamma model belongs to the exponential family. We used the following transformations to improve the quality of the normal approximations for moderate  $n$ :  $\theta = \log(\theta_1) - \log(\theta_2)$  and  $\boldsymbol{\eta}_j = (\log(\alpha_j), \log(\beta_j))$  for  $j = 1, 2$ . We then selected an appropriate array of sample sizes  $n$ . For each value of  $n$ , we generated 10000 samples of that size from  $f(y; \boldsymbol{\eta}_{1,0})$  and  $f(y; \boldsymbol{\eta}_{2,0})$ . We approximated the corresponding posterior of  $\theta = \theta_1/\theta_2$  using MCMC methods and determined whether  $100 \times \gamma\%$  of the posterior was contained within  $(\delta_L, \delta_U)$ . For each  $n$  explored, we computed the proportion of the 10000 samples in which this occurred to approximate the power curve. Figure 2 depicts these results.

For all settings considered, the alignment between the blue and red curves in Figure 2 indicates that the power curves generated by our method with Algorithm 2 perform well. The root-finding algorithm has

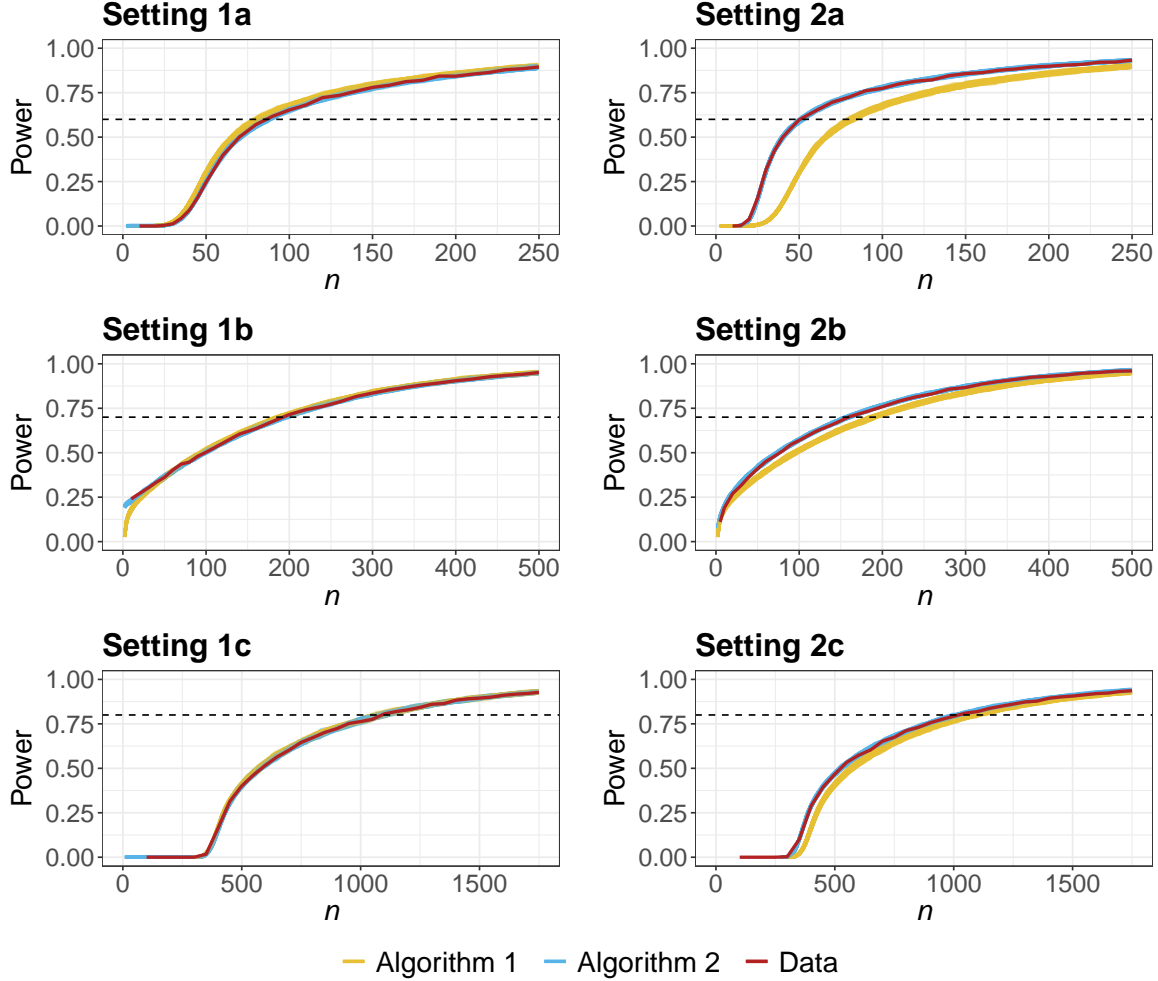


Figure 2: 100 power curves obtained via Algorithms 1 (yellow) and 2 (blue), power curve estimated via simulated data (red), and target power  $\Gamma$  (dotted line) for each setting with hypothesis tests facilitated via posterior probabilities.

not led to performance issues – even with moderate sample sizes. In total, we approximated 2800 power curves for the gamma tail probability example in this section and Appendix D of the supplement. We did not need to reinitialize the root-finding algorithm in Lines 9 to 15 of Algorithm 4 for *any* of the  $2.867 \times 10^6$  points used to generate these 2800 curves. The power curves obtained using our method with Algorithm 1 require large sample sizes  $n$  or uninformative priors to yield good performance. This is evident as the yellow curves do not approximate the red curves for the settings with informative priors. Even in Setting 1a with uninformative priors and moderate sample sizes, the yellow power curves are noticeably shifted to the left. The bias is a result of the approximation in (8) not accounting for the priors and not the root-finding algorithm. Algorithm 2 also performs better for smaller sample sizes in Setting 1b as the sample sizes corresponding to low power are too small for the BvM theorem to be invoked. For Setting 1c, neither the blue nor yellow power curves differ substantially from the red curve. This is a direct consequence of the BvM theorem.

Each yellow power curve in Figure 2 was estimated in 2 to 3 seconds without parallelization, whereas each blue curve took roughly 5 seconds to approximate without parallelization. The blue curves take slightly longer to estimate because we must find the posterior modes  $\tilde{\eta}_{1,n}$  and  $\tilde{\eta}_{2,n}$  using optimization methods. We therefore recommend using Algorithm 4 with the posterior approximation method from Algorithm 2 whenever possible since this method accounts for the prior distributions without a substantial increase in runtime. With the same computational resources for this example, we can approximate a handful of posteriors using standard computational methods. This is not sufficient to produce even a crude power estimate for a single sample size  $n$ .

Because power curve approximation for hypothesis tests with Bayes factors just requires that we choose  $\gamma$  to align with the right side of (5), we consider the performance of our method for such analyses in Appendix D.1 of the supplement. We now reconsider Settings 1a and 2a with analyses facilitated via equal-tailed credible intervals. We choose  $\alpha = 1 - \gamma = 0.4$  for this analysis. We again implemented Algorithm 4 with  $\zeta = \{\text{Alg. 1}, \text{Alg. 2}\}$  to obtain 100 power curves with each method. When approximating the power curve by simulating data, we computed power as the proportion of simulation repetitions in which  $100 \times (1 - \alpha/2)\%$  of the posterior for  $\theta = \theta_1/\theta_2$  was contained within each of the following intervals:  $(\delta_L, \infty)$  and  $(-\infty, \delta_U)$ . These results for Settings 1a and 2a are visualized in Figure 3.

For analyses with credible intervals, we draw similar conclusions about the performance of our approach with Algorithms 1 and 2 as in Figure 2. Each blue curve in Figure 3 took roughly 7 seconds to estimate since we must examine the intervals corresponding to two one-sided tests with posterior probabilities as discussed in Section 4.2. Because sufficient statistics can be readily computed for this example, we did not consider the performance of our approach to power analysis with the approximation method in Algorithm 3. We consider the performance of that approach in Section 5.2.

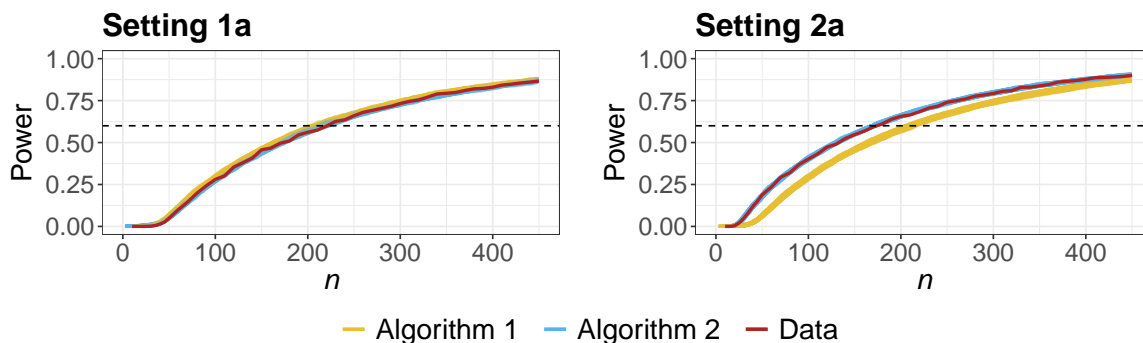


Figure 3: 100 power curves obtained via Algorithms 1 (yellow) and 2 (blue), power curve estimated via simulated data (red), and target power  $\Gamma$  (dotted line) for Settings 1a and 2a with hypothesis tests facilitated via credible intervals.

## 5.2 Power Curve Approximation with the Weibull Distribution

To further explore the performance of our power curve approximation procedure, we reconsider the food expenditure example with Weibull distributions. We find design values for the Weibull distributions using the data from the ENIGH 2018 survey processed in Section 5.1. We find the posterior means for the Weibull shape and scale parameters to be  $\bar{\nu}_1 = 1.41$  and  $\bar{\lambda}_1 = 3.39$  for the female provider group and  $\bar{\nu}_2 = 1.49$  and  $\bar{\lambda}_2 = 3.42$  for the male provider group, where GAMMA(2, 1) priors were assigned to each parameter. These posterior means comprise the new design values  $\boldsymbol{\eta}_{1,0}$  and  $\boldsymbol{\eta}_{2,0}$ . As in Section 5.1, a threshold of  $\kappa_0 = 4.29$  defines the Weibull tail probabilities.

We again consider two sets of prior distributions. For the first set, we specify uninformative GAMMA(2, 1) priors for the Weibull parameters  $\nu_j$  and  $\lambda_j$  for group  $j = 1, 2$ . To choose the second set of priors, we reconsider the approximately gamma distributed posteriors used to obtain design values for  $\nu_1$ ,  $\lambda_1$ ,  $\nu_2$ , and  $\lambda_2$ . To incorporate prior information, we consider gamma distributions that have the same modes with variances that are larger by a factor of 100. These distributions prompt the following informative priors: GAMMA(12.73, 8.28) for  $\nu_1$ , GAMMA(11.81, 3.20) for  $\lambda_1$ , GAMMA(38.35, 25.09) for  $\nu_2$ , and GAMMA(37.91, 10.79) for  $\lambda_2$ . For each prior specification, we consider power curve estimation for analyses facilitated via posterior probabilities with Settings 1a and 2a from Section 5.1, where  $((\delta_L, \delta_U), \gamma, \Gamma) = ((1.25^{-1}, 1.25), 0.5, 0.6)$ . For each setting, we generated 100 power curves using Algorithm 4 with  $\zeta = \{\text{Alg. 1, Alg. 3}\}$ . We used the following transformations to improve the quality of the normal approximations:  $\theta = \log(\theta_1) - \log(\theta_2)$  and  $\boldsymbol{\eta}_j = (\log(\nu_j), \log(\lambda_j))$  for  $j = 1, 2$ . As in Section 5.1, we also estimated the power curves by generating data from the design distributions and approximating the posterior of  $\theta = \theta_1/\theta_2$ . Figure 4 depicts these results.

For Settings 1a and 2a, we draw similar conclusions for the blue and yellow power curves as in Figure 2 with the gamma model. Algorithm 3 therefore yields suitable performance for this example when low-dimensional sufficient statistics cannot be calculated. Each yellow and blue power curve in Figure 4 was

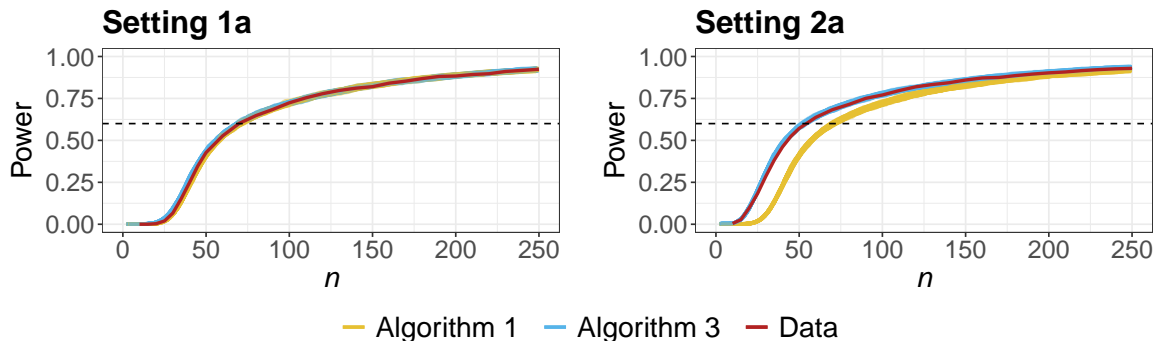


Figure 4: 100 power curves obtained via Algorithms 1 (yellow) and 3 (blue), power curve estimated via simulated data (red), and target power  $\Gamma$  (dotted line) for Settings 1a and 2a with hypothesis tests using the Weibull distribution.

estimated in less than five seconds without parallelization. For this example with the Weibull model, we cannot approximate a single posterior of  $\theta$  using the same computing resources. While our power curve approximation method does not require parallel computing for fast performance, all power curves in our numerical studies could be estimated in a second or two if parallelized on a standard laptop with four cores. As such, our method for power curve approximation allows users to quickly explore potential designs for their study in real time, expediting communication between stakeholders of the study.

## 6 Discussion

In this paper, we developed a framework for fast power curve approximation with hypothesis tests facilitated via posterior probabilities, Bayes factors, and credible intervals. The computational efficiency of this framework stems from a targeted approach to explore the sampling distribution of posterior probabilities for each sample size considered when the conditions for the BvM theorem are satisfied. The numerical studies conducted show that our fast method yields suitable power curve approximation for moderate and large sample sizes. While this method is not appropriate for small sample sizes, it informs practitioners when their required sample sizes are small. More traditional simulation-based design methods can be used in these scenarios since they are often less cumbersome to implement with small sample sizes.

It may be possible to make this framework more flexible by extending it to the predictive approach for choosing the sampling distribution of  $\mathbf{Y}^{(n)}$ . This would prevent us from directly applying the BvM theorem. However, perhaps results from the BvM theorem (where we treat a draw from the design prior as the fixed parameter  $\boldsymbol{\eta}_{j,0}$ ) could be combined with targeted sampling techniques to yield fast sample size recommendations. This framework could also be extended to accommodate multiple study objectives. For instance, we may require a sample size  $n$  that both satisfies a power criterion and bounds a type I error or false discovery rate.

Moreover, the framework presented in the main paper does not support imbalanced two-group sample size determination (i.e., where  $n_2 = qn_1$  for some constant  $q > 0$ ). It may be inefficient or impractical to force  $q = 1$  when prior information for one group is much more precise, when it is more difficult to sample from one of the groups, or in scenarios where one treatment is much riskier. In Appendix D.2 of the supplement, we extend this framework to settings where practitioners specify this constant  $q$ .

## Supplementary Material

These materials include a detailed description of the conditions for Theorem 1 and Lemma 1 along with their proofs and additional simulation results. The code to implement Algorithm 4 and conduct the numerical studies in the main paper is available online: <https://github.com/lmhagar/BayesianPower>.

## Funding Acknowledgement

This work was supported by the Natural Sciences and Engineering Research Council of Canada (NSERC) by way of CGS M and PGS D scholarships as well as Grant RGPIN-2019-04212.

## References

- Berry, S. M., B. P. Carlin, J. J. Lee, and P. Muller (2011). *Bayesian Adaptive Methods for Clinical Trials*. CRC press.
- Brent, R. P. (1973). An algorithm with guaranteed convergence for finding the minimum of a function of one variable. *Algorithms for Minimization without Derivatives, Prentice-Hall, Englewood Cliffs, NJ*, 61–80.
- Brutti, P., F. De Santis, and S. Gubbiotti (2014). Bayesian-frequentist sample size determination: a game of two priors. *Metron* 72(2), 133–151.
- Chaloner, K. (1996). Elicitation of prior distributions. In *Bayesian biostatistics*, pp. 141–156. Marcel Dekker, New York.
- De Santis, F. (2007). Using historical data for Bayesian sample size determination. *Journal of the Royal Statistical Society: Series A (Statistics in Society)* 170(1), 95–113.
- Garthwaite, P. H., J. B. Kadane, and A. O’Hagan (2005). Statistical methods for eliciting probability distributions. *Journal of the American Statistical Association* 100(470), 680–701.
- Gelman, A., J. B. Carlin, H. S. Stern, D. B. Dunson, A. Vehtari, and D. B. Rubin (2013). *Bayesian Data Analysis*. CRC press.
- Gubbiotti, S. and F. De Santis (2011). A bayesian method for the choice of the sample size in equivalence trials. *Australian & New Zealand Journal of Statistics* 53(4), 443–460.
- Hagar, L. and N. T. Stevens (2023). Supplement to “fast sample size determination for Bayesian equivalence tests”. *Bayesian Analysis* (submitted).
- Hofert, M. and C. Lemieux (2020). *qrng: (Randomized) Quasi-Random Number Generators*. R package version 0.0-8.
- Instituto Nacional de Estadística, Geografía e Informática [National Institute of Statistics, Geography, and Informatics] (INEGI) (2019). Encuesta Nacional de Ingresos y Gastos de los Hogares (ENIGH). 2018 Nueva serie [National Survey of Household Income and Expenses. New edition 2018]. [www.inegi.org.mx/programas/enigh/nc/2018/#Datos\\_abiertos](http://www.inegi.org.mx/programas/enigh/nc/2018/#Datos_abiertos).

- Instituto Nacional de Estadística, Geografía e Informática [National Institute of Statistics, Geography, and Informatics] (INEGI) (2021). Encuesta Nacional de Ingresos y Gastos de los Hogares (ENIGH). 2020 Nueva serie [National Survey of Household Income and Expenses. New edition 2020]. [www.inegi.org.mx/programas/enigh/nc/2020/#Datos\\_abiertos](http://www.inegi.org.mx/programas/enigh/nc/2020/#Datos_abiertos).
- Jeffreys, H. (1935). Some tests of significance, treated by the theory of probability. In *Mathematical Proceedings of the Cambridge Philosophical Society*, Volume 31, pp. 203–222. Cambridge University Press.
- Johnson, S. R., G. A. Tomlinson, G. A. Hawker, J. T. Granton, and B. M. Feldman (2010). Methods to elicit beliefs for Bayesian priors: a systematic review. *Journal of clinical epidemiology* 63(4), 355–369.
- Kass, R. E. and A. E. Raftery (1995). Bayes factors. *Journal of the American Statistical Association* 90(430), 773–795.
- Kruschke, J. K. (2018). Rejecting or accepting parameter values in Bayesian estimation. *Advances in Methods and Practices in Psychological Science* 1(2), 270–280.
- Lehmann, E. L. and G. Casella (1998). *Theory of Point Estimation*. Springer Science & Business Media.
- Lemieux, C. (2009). Using quasi–monte carlo in practice. In *Monte Carlo and Quasi-Monte Carlo Sampling*, pp. 1–46. Springer.
- Morey, R. D. and J. N. Rouder (2011). Bayes factor approaches for testing interval null hypotheses. *Psychological methods* 16(4), 406.
- Sobol', I. M. (1967). On the distribution of points in a cube and the approximate evaluation of integrals. *Zhurnal Vychislitel'noi Matematiki i Matematicheskoi Fiziki* 7(4), 784–802.
- Spiegelhalter, D. J., K. R. Abrams, and J. P. Myles (2004). *Bayesian approaches to clinical trials and health-care evaluation*, Volume 13. John Wiley & Sons.
- Spiegelhalter, D. J., L. S. Freedman, and M. K. Parmar (1994). Bayesian approaches to randomized trials. *Journal of the Royal Statistical Society: Series A (Statistics in Society)* 157(3), 357–387.
- Stevens, N. T. and L. Hagar (2022). Comparative probability metrics: Using posterior probabilities to account for practical equivalence in A/B tests. *The American Statistician* 76(3), 224–237.
- van der Vaart, A. W. (1998). *Asymptotic Statistics*. Cambridge Series in Statistical and Probabilistic Mathematics. Cambridge University Press.
- Wang, F. and A. E. Gelfand (2002). A simulation-based approach to bayesian sample size determination for performance under a given model and for separating models. *Statistical Science* 17(2), 193–208.

# Supplementary Material for Fast Power Curve Approximation for Posterior Analyses

## A Additional Content for Theorem 1

### A.1 Conditions for the Bernstein-von Mises Theorem

Theorem 1 from the main text requires that the conditions for the Bernstein-von Mises (BvM) theorem are satisfied. These conditions are described in more detail in [van der Vaart \(1998\)](#), starting on page 140. Conditions (B0), (B1), and (B2) concern the likelihood component of the posterior distribution for a parameter  $\theta$ . (B3) concerns the prior specifications for  $\theta$ .

- (B0) The observations are drawn independently and identically from a distribution  $P_{\theta_0}$  for some fixed, nonrandom  $\theta_0$ .
- (B1) The parametric statistical model from which the data are generated is differentiable in quadratic mean.
- (B2) There exists a sequence of uniformly consistent tests for testing  $H_0 : \theta = \theta_0$  against  $H_1 : \|\theta - \theta_0\| \geq \varepsilon$  for every  $\varepsilon > 0$ .
- (B3) Let the prior distribution for  $\theta$  be absolutely continuous in a neighbourhood of  $\theta_0$  with continuous positive density at  $\theta_0$ .

### A.2 Conditions for the Asymptotic Normality of the Maximum Likelihood Estimator

Theorem 1 from the main text also requires that the design distributions  $f(y; \boldsymbol{\eta}_{1,0})$  and  $f(y; \boldsymbol{\eta}_{2,0})$  satisfy the regularity conditions for the asymptotic normality of the maximum likelihood estimator. These conditions are detailed in [Lehmann and Casella \(1998\)](#); they consider a family of probability distributions  $\mathcal{P} = \{P_\theta : \theta \in \Omega\}$ , where  $\Omega$  is the parameter space. [Lehmann and Casella \(1998\)](#) use  $\theta$  as the unknown parameter with true fixed value  $\theta_0$ , so we state the conditions using this notation. However, we use  $\theta = \theta_1 - \theta_2$  or  $\theta = \theta_1/\theta_2$  to compare two characteristics in our framework. For our purposes, the conditions in [Lehmann and Casella \(1998\)](#) must hold for the design distributions (with unknown parameters  $\boldsymbol{\eta}_1$  and  $\boldsymbol{\eta}_2$  and true values  $\boldsymbol{\eta}_{1,0}$  and  $\boldsymbol{\eta}_{2,0}$ ).

[Lehmann and Casella \(1998\)](#) detail nine conditions that guarantee the asymptotic normality of the maximum likelihood estimator. We provide the following guidance on where to find more information about

these conditions in their text. The first four conditions – (R0), (R1), (R2), and (R3) – are described on pages 443 and 444 of their text. (R4) is mentioned as part of Theorem 3.7 on page 447. (R5), (R6), and (R7) are described in Theorem 2.6 on pages 440 and 441. (R8) is mentioned in Theorem 3.10 on page 449.

(R0) The distributions  $P_\theta$  of the observations are distinct.

(R1) The distributions  $P_\theta$  have common support.

(R2) The observations are  $\mathbf{X} = (X_1, \dots, X_n)$ , where the  $X_i$  are identically and independently distributed with probability density function  $f(x_i|\theta)$  with respect to a  $\sigma$ -finite measure  $\mu$ .

(R3) The parameter space  $\Omega$  contains an open set  $\omega$  of which the true parameter value  $\theta_0$  is an interior point.

(R4) For almost all  $x$ ,  $f(x|\theta)$  is differentiable with respect to  $\theta$  in  $\omega$ , with derivative  $f'(x|\theta)$ .

(R5) For every  $x$  in the set  $\{x : f(x|\theta) > 0\}$ , the density  $f(x|\theta)$  is differentiable up to order 3 with respect to  $\theta$ , and the third derivative is continuous in  $\theta$ .

(R6) The integral  $\int f(x|\theta)d\mu(x)$  can be differentiated three times under the integral sign.

(R7) The Fisher information  $\mathcal{I}(\theta)$  satisfies  $0 < \mathcal{I}(\theta) < \infty$ .

(R8) For any given  $\theta_0 \in \Omega$ , there exists a positive number  $c$  and a function  $M(x)$  (both of which may depend on  $\theta_0$ ) such that  $|\partial^3 \log f(x|\theta) / \partial \theta^3| \leq M(x)$  for all  $\{x : f(x|\theta) > 0\}$ ,  $\theta_0 - c < \theta < \theta_0 + c$ , and  $\mathbb{E}[M(X)] < \infty$ .

### A.3 Proof of Theorem 1

We first prove part (a) of Theorem 1. When data  $\mathbf{Y}^{(n)}$  are generated, the fraction inside the standard normal CDF of (3.6) in the main text with the posterior approximation method from (3.1) converges to the following normal distribution:

$$\sqrt{n} \left( \frac{\delta - \theta_0}{\sqrt{\mathcal{I}(\hat{\theta}_n)^{-1}}} - \frac{\hat{\theta}_n - \theta_0}{\sqrt{\mathcal{I}(\hat{\theta}_n)^{-1}}} \right) \xrightarrow{d} \mathcal{N} \left( \frac{\delta - \theta_0}{\sqrt{\mathcal{I}(\theta_0)^{-1}}}, 1 \right). \quad (\text{A.1})$$

This result follows by the asymptotic normality of the MLEs  $\hat{\eta}_{1,n}$  and  $\hat{\eta}_{2,n}$ , the continuous mapping theorem because  $g(\cdot)$  and  $h(\cdot)$  are differentiable at the design values, and Slutsky's theorem since  $\mathcal{I}(\hat{\theta}_n)^{-1} \xrightarrow{P} \mathcal{I}(\theta_0)^{-1}$ . When pseudorandom sequences  $\mathbf{U} \stackrel{\text{i.i.d.}}{\sim} \mathcal{U}([0, 1]^{2d})$  are input into Algorithm 1, the left side of (A.1) follows the normal distribution on the right side exactly. We directly obtain the result in part (a) by a second application of the continuous mapping theorem with the function  $\Phi(\cdot)$ .

To prove part (b), we note that the approximations in (3.1) and (3.2) of the main text are virtually the same as  $n \rightarrow \infty$ . Under the conditions for Theorem 1, the posterior mode  $\tilde{\eta}_{j,n}$  converges in probability to

$\boldsymbol{\eta}_{j,0}$  for  $j = 1, 2$ . The following result also holds for  $\mathcal{J}_j(\tilde{\boldsymbol{\eta}}_{j,n})/n$  in (3.2) of the main text:

$$\frac{1}{n}\mathcal{J}_j(\tilde{\boldsymbol{\eta}}_{j,n}) = \left[ -\frac{1}{n} \sum_{i=1}^n \frac{\partial^2}{\partial \boldsymbol{\eta}_j^2} \log(f(y_{ij}; \boldsymbol{\eta}_j)) - \frac{1}{n} \frac{\partial^2}{\partial \boldsymbol{\eta}_j^2} \log(p_j(\boldsymbol{\eta}_j)) \right]_{\boldsymbol{\eta}_j = \tilde{\boldsymbol{\eta}}_{j,n}} \xrightarrow{P} \mathcal{I}(\boldsymbol{\eta}_{j,0}). \quad (\text{A.2})$$

Because  $\tilde{\boldsymbol{\eta}}_{j,n} - \hat{\boldsymbol{\eta}}_{j,n} \xrightarrow{P} 0$ , the mean and variance of the normal distribution in (3.2) of the main text respectively approximate  $\hat{\boldsymbol{\theta}}_n$  and  $\mathcal{I}(\hat{\boldsymbol{\theta}}_n)/n$  in (3.1) for large sample sizes  $n$  by the continuous mapping theorem. The result in part (b) then follows from part (a).  $\square$

## B Proof of Lemma 1

To prove part (a) of Lemma 1 from the main text, we only present the proof for group 1 since the proof for group 2 follows the same process. We use induction on the dimension  $d$  of  $\boldsymbol{\eta}_1$  for this proof. We show the base case corresponding to a model with  $d = 2$ . To simplify notation, we let

$$\mathcal{I}(\boldsymbol{\eta}_{1,0})^{-1} = \begin{bmatrix} \sigma_{11}^2 & \rho_{12}\sigma_{11}\sigma_{22} \\ \rho_{12}\sigma_{11}\sigma_{22} & \sigma_{22}^2 \end{bmatrix}.$$

By properties of the bivariate conditional normal distribution, it follows that

$$\hat{\boldsymbol{\eta}}_{1,n}(\mathbf{u}_r)^{(1)} = \boldsymbol{\eta}_{1,0}^{(1)} + \frac{1}{\sqrt{n}}\Phi^{-1}(u_1)\sigma_{11} \quad \text{and} \quad (\text{B.1})$$

$$\hat{\boldsymbol{\eta}}_{1,n}(\mathbf{u}_r)^{(2)} = \boldsymbol{\eta}_{1,0}^{(2)} + \frac{1}{\sqrt{n}}\sigma_{22} \left[ \Phi^{-1}(u_1)\rho_{12} + \Phi^{-1}(u_2)\sqrt{1 - \rho_{12}^2} \right]. \quad (\text{B.2})$$

The result in part (a) therefore holds true when  $d = 2$ , where  $\omega_1(u_1)$  and  $\omega_2(u_1, u_2)$  are given by the expressions to the right of the  $1/\sqrt{n}$  terms in (B.1) and (B.2), respectively.

For the inductive hypothesis, we assume that the result in part (a) of Lemma 1 holds true for a model with  $d = l$  parameters. For the inductive conclusion, we show that this implies the result also holds for a model with  $d = l + 1$  parameters. Because  $\hat{\boldsymbol{\eta}}_{1,n}(\mathbf{u}_r)^{(1)}, \dots, \hat{\boldsymbol{\eta}}_{1,n}(\mathbf{u}_r)^{(l)}$  only depend on the components with smaller indices, we just need to prove that the result in part (a) holds for  $\hat{\boldsymbol{\eta}}_{1,n}(\mathbf{u}_r)^{(l+1)}$ . That result in conjunction with the inductive hypothesis proves the inductive conclusion. To prove the inductive conclusion, we introduce the following block matrix notation:

$$\mathcal{I}(\boldsymbol{\eta}_{1,0})^{-1} = \begin{bmatrix} \boldsymbol{\Sigma}_{l,l} & \boldsymbol{\Sigma}_{l,1} \\ \boldsymbol{\Sigma}_{1,l} & \Sigma_{l+1,l+1} \end{bmatrix},$$

where  $\boldsymbol{\Sigma}_{l,l}$  is a  $l \times l$  matrix,  $\boldsymbol{\Sigma}_{l,1}$  is a  $l \times 1$  matrix,  $\boldsymbol{\Sigma}_{1,l} = \boldsymbol{\Sigma}_{l,1}^T$ , and  $\Sigma_{l+1,l+1}$  is scalar.

The marginal distribution of  $\hat{\boldsymbol{\eta}}_{1,n}^{(l+1)}$  conditional on the already-generated  $\hat{\boldsymbol{\eta}}_{1,n}(\mathbf{u}_r)^{(k)}$  for  $k = 1, \dots, l$  is

$$\mathcal{N} \left( \boldsymbol{\eta}_{1,0}^{(l+1)} + \frac{1}{\sqrt{n}} \boldsymbol{\Sigma}_{1,l} \boldsymbol{\Sigma}_{l,l}^{-1} \begin{pmatrix} \omega_1(u_1) \\ \vdots \\ \omega_l(u_1, \dots, u_l) \end{pmatrix}, \frac{1}{n} \left[ \Sigma_{l+1,l+1} - \boldsymbol{\Sigma}_{1,l} \boldsymbol{\Sigma}_{l,l}^{-1} \boldsymbol{\Sigma}_{l,1} \right] \right).$$

Therefore, we have that

$$\begin{aligned} \hat{\boldsymbol{\eta}}_{1,n}(\mathbf{u}_r)^{(l+1)} &= \boldsymbol{\eta}_{1,0}^{(l+1)} + \frac{1}{\sqrt{n}} \boldsymbol{\Sigma}_{1,l} \boldsymbol{\Sigma}_{l,l}^{-1} \begin{pmatrix} \omega_1(u_1) \\ \vdots \\ \omega_l(u_1, \dots, u_l) \end{pmatrix} \\ &+ \frac{1}{\sqrt{n}} \Phi^{-1}(u_{l+1}) \left[ \boldsymbol{\Sigma}_{l+1,l+1} - \boldsymbol{\Sigma}_{1,l} \boldsymbol{\Sigma}_{l,l}^{-1} \boldsymbol{\Sigma}_{l,1} \right]. \end{aligned} \quad (\text{B.3})$$

The result from part (a) of Lemma 1 holds for  $\hat{\boldsymbol{\eta}}_{1,n}(\mathbf{u}_r)^{(l+1)}$  if we take  $\omega_{l+1}(u_1, \dots, u_{l+1})$  as the sum of the two components to the right of the  $1/\sqrt{n}$  terms in (B.3). By mathematical induction, part (a) of Lemma 1 of the main text is true for an arbitrary model with  $d$  parameters.

Part (b) of Lemma 1 follows from the first-order Taylor expansion of  $h(g(\hat{\boldsymbol{\eta}}_{1,n}(\mathbf{u}_r)), g(\hat{\boldsymbol{\eta}}_{2,n}(\mathbf{u}_r)))$  around  $(\boldsymbol{\eta}_{1,0}, \boldsymbol{\eta}_{2,0})$ . We have that

$$\begin{aligned} &h(g(\hat{\boldsymbol{\eta}}_{1,n}(\mathbf{u}_r)), g(\hat{\boldsymbol{\eta}}_{2,n}(\mathbf{u}_r))) - h(g(\boldsymbol{\eta}_{1,0}), g(\boldsymbol{\eta}_{2,0})) \\ &\approx \sum_{j=1}^2 \sum_{k=1}^d \frac{\partial h}{\partial g_j} \frac{\partial g_j}{\partial \boldsymbol{\eta}_j^{(k)}} \Big|_{(\boldsymbol{\eta}_1, \boldsymbol{\eta}_2) = (\boldsymbol{\eta}_{1,0}, \boldsymbol{\eta}_{2,0})} \left[ \hat{\boldsymbol{\eta}}_{j,n}(\mathbf{u}_r)^{(k)} - \boldsymbol{\eta}_{j,0}^{(k)} \right] \\ &\approx \frac{1}{\sqrt{n}} \left[ \sum_{j=1}^2 \sum_{k=1}^d \frac{\partial h}{\partial g_j} \frac{\partial g_j}{\partial \boldsymbol{\eta}_j^{(k)}} \Big|_{(\boldsymbol{\eta}_1, \boldsymbol{\eta}_2) = (\boldsymbol{\eta}_{1,0}, \boldsymbol{\eta}_{2,0})} \omega_{(j-1)d+k}(u_{(j-1)d+1}, \dots, u_{(j-1)d+k}) \right]. \end{aligned} \quad (\text{B.4})$$

Part (b) of Lemma 1 follows if we let  $\omega_{\dagger}(\cdot)$  be the sum on the right side of the  $1/\sqrt{n}$  term in (B.4). However, this Taylor series expansion may only be suitable for large sample sizes  $n$  – when  $\hat{\boldsymbol{\eta}}_{j,n}(\mathbf{u}_r)$  is sufficiently near  $\boldsymbol{\eta}_{j,0}$  for  $j = 1, 2$ . Our simulation procedure for  $\hat{\boldsymbol{\eta}}_{j,n}(\mathbf{u}_r)$  ensures this convergence occurs for large  $n$ , and the conditions for Theorem 1 of the main text guarantee that  $\hat{\boldsymbol{\eta}}_{j,n}$  based on the data  $\mathbf{y}^{(n)}$  also converges in probability to  $\boldsymbol{\eta}_{j,0}$ .

To prove part (c), we note that the following result holds for sufficiently large  $n$ :

$$\begin{aligned} \frac{\delta - \underline{\theta}_r^{(n)}}{\sqrt{\mathcal{I}_r^{(n)}}} &\approx \frac{\delta - (h(g(\boldsymbol{\eta}_{1,0}), g(\boldsymbol{\eta}_{2,0}))) + \omega_{\dagger}(u_1, \dots, u_{2d})/\sqrt{n}}{\sqrt{\mathcal{I}(\theta_0)^{-1}/n}} \\ &= \frac{\delta - \theta_0}{\sqrt{\mathcal{I}(\theta_0)^{-1}}} \sqrt{n} + \frac{\omega_{\dagger}(u_1, \dots, u_{2d})}{\sqrt{\mathcal{I}(\theta_0)^{-1}}}. \end{aligned} \quad (\text{B.5})$$

The approximate equivalence of the numerators in the first line of (B.5) follows from part (b) of Lemma 1 and the fact that  $\tilde{\boldsymbol{\eta}}_{j,n} - \hat{\boldsymbol{\eta}}_{j,n}$  and  $\boldsymbol{\eta}_{j,n}^* - \hat{\boldsymbol{\eta}}_{j,n}$  converge in probability to 0 as mentioned in the main text. Moreover,  $\mathcal{I}_r^{(n)} \approx \mathcal{I}(\theta_0)^{-1}/n$  for sufficiently large  $n$  by the continuous mapping theorem for Algorithm 1, (A.2) for Algorithm 2, and similar logic to (A.2) for Algorithm 3. The second line of (B.5) holds because  $\theta_0 = h(g(\boldsymbol{\eta}_{1,0}), g(\boldsymbol{\eta}_{2,0}))$ . The expression in (B.5) takes the form  $a(\delta, \theta_0)\sqrt{n} + b(\mathbf{u}_r)$  since neither fraction in the second line depends on  $n$ . Part (c) of Lemma 1 follows by using the normal CDF as in (3.6) of the main text. We note that the function  $a(\delta, \theta_0)$ , which is the fraction to the left of the  $\sqrt{n}$  term in the second line of (B.5), must incorporate monotonic transformations applied to the posterior of  $\theta$  to improve the suitability of its normal approximation.

Part (d) of Lemma 1 follows from taking the derivative of the approximation to  $p_{n,\mathbf{u}_r,\zeta}^{\delta_U} - p_{n,\mathbf{u}_r,\zeta}^{\delta_L}$  prompted by part (c) with respect to the sample size  $n$ :

$$\begin{aligned} & \frac{d}{dn} \left[ p_{n,\mathbf{u}_r,\zeta}^{\delta_U} - p_{n,\mathbf{u}_r,\zeta}^{\delta_L} \right] \\ & \approx \frac{d}{dn} \left[ \Phi \left( a(\delta_U, \theta_0) \sqrt{n} + b(\mathbf{u}_r) \right) - \Phi \left( a(\delta_L, \theta_0) \sqrt{n} + b(\mathbf{u}_r) \right) \right] \\ & = \frac{a(\delta_U, \theta_0) \phi \left( a(\delta_U, \theta_0) \sqrt{n} + b(\mathbf{u}_r) \right) - a(\delta_L, \theta_0) \phi \left( a(\delta_L, \theta_0) \sqrt{n} + b(\mathbf{u}_r) \right)}{2\sqrt{n}}, \end{aligned} \tag{B.6}$$

where  $\phi(\cdot)$  is the probability density function (PDF) of the standard normal distribution. This derivative must be positive for sufficiently large  $n$  where the approximation from part (c) of Lemma 1 holds. When  $\theta_0 \in (\delta_L, \delta_U)$ ,  $a(\delta_U, \theta_0)$  is positive and  $a(\delta_L, \theta_0)$  is negative. Because the normal distribution takes support over the entire real line,  $\phi(\cdot)$  returns a positive value for any real input. If  $\delta_L$  or  $\delta_U$  is not finite, then its component of the difference in the numerator of (B.6) is zero. The remaining component of the numerator is still positive and so is the derivative in (B.6). Hence, part (d) of Lemma 1 is true, and  $p_{n,\mathbf{u}_r,\zeta}^{\delta_U} - p_{n,\mathbf{u}_r,\zeta}^{\delta_L}$  is an increasing function for sufficiently large  $n$ .  $\square$

## C Additional Content for Alternatives to Pseudorandom Sampling

### C.1 Visualization of Targeted Sampling Procedure

The motivating example with gamma tail probabilities from Section 2 of the main text has dimension of  $2d = 4$  since we consider the posteriors of  $\boldsymbol{\eta}_j = (\alpha_j, \beta_j)$  for  $j = 1, 2$ . In this section, we consider a two-dimensional example involving the comparison of Bernoulli proportions that is easier to visualize. Even though this model has a conjugate prior, it is considered for illustrative purposes. We let  $\theta_j$  be the Bernoulli success probability for model  $j = 1, 2$ . For this example, we let  $\eta_j = \log(\theta_j) - \log(1 - \theta_j)$  to improve the quality of the normal approximations to the posterior for  $\eta_j$  and the sampling distribution of its MLE. This simple transformation is based on the canonical form of the standard Bernoulli model (Lehmann and Casella, 1998).

We compare the Bernoulli probabilities via their difference:  $\theta_1 - \theta_2$ . Because  $\theta_1 - \theta_2 \in (-1, 1)$ , we similarly consider the posterior distribution of  $\log(\theta_1 - \theta_2 + 1) - \log(1 - \theta_1 + \theta_2)$  to improve the quality of the normal approximations for moderate  $n$ . The selected transformation for  $\theta$  is a straightforward generalization of the transformation applied to each  $\eta_j$  parameter. An alternative monotonic transformation could have been chosen to minimize the Kullback-Leibler divergence (Gelman et al., 2013) for the normal approximation to the posterior. However, the optimal transformation likely depends on the sample size and the data generated from the design distributions. Any transformations such that  $\boldsymbol{\eta}_1$  and  $\boldsymbol{\eta}_2$  have support over  $\mathbb{R}^d$  and  $\theta$  has support over the entire real line are suitable in the limiting case. To streamline our methods, we suggest using visualization techniques to compare the suitability of several candidate monotonic transformations if

necessary.

We choose design values of  $\theta_{1,0} = 0.15$  and  $\theta_{2,0} = 0.14$ , which gives rise to design values  $\eta_{1,0}$  and  $\eta_{2,0}$  on the logit scale. The scenarios we consider are based on two sets of prior distributions. For the first set, we specify uninformative  $\text{BETA}(1, 1)$  priors for the Bernoulli parameters  $\theta_1$  and  $\theta_2$ . These conjugate beta priors induce priors on the variables  $\eta_1$  and  $\eta_2$ . We also consider a set of informative priors for the Bernoulli parameters:  $\text{BETA}(3.75, 21.25)$  for  $\theta_1$  and  $\text{BETA}(3.50, 21.50)$  for  $\theta_2$ . These beta distributions have modes that roughly align with the design values  $\theta_{1,0}$  and  $\theta_{2,0}$ . For both sets of priors, we consider power curve approximation for analyses with posterior probabilities, where  $(\delta_L, \delta_U) = (-0.05, 0.05)$  on the probability scale,  $\gamma = 0.8$ , and  $\Gamma = 0.6$ .

We consider the posterior approximation method in Algorithm 1 from the main text for Setting 1a with uninformative priors. For Setting 2a with informative priors, we consider the posterior approximation method from Algorithm 2. Figure C.1 visualizes how points from  $[0, 1]^2$  are explored in the second round of the root-finding procedure from Algorithm 4 for each setting. We used the same Sobol' sequence of length  $m = 1024$  for both settings to facilitate comparison. We note that the entire point set in  $[0, 1]^2$  comprised of the grey and red points does not resemble random scatter over the unit square. Distinct patterns are observed in the point set because the low-discrepancy Sobol' sequences induce negative dependence between the points.

For both Setting 1a and 2a, the root-finding algorithm is initialized at  $\lceil n_0 \rceil = 300$ . Therefore, all points in Figure C.1 are used to explore that sample size. This is close to the final sample size recommendation of  $\lceil n^* \rceil = 305$  for Setting 1a. Only the grey points at which  $p_{300, \mathbf{u}_r, \zeta}^{\delta_U} - p_{300, \mathbf{u}_r, \zeta}^{\delta_L} \geq \gamma$  were used to explore

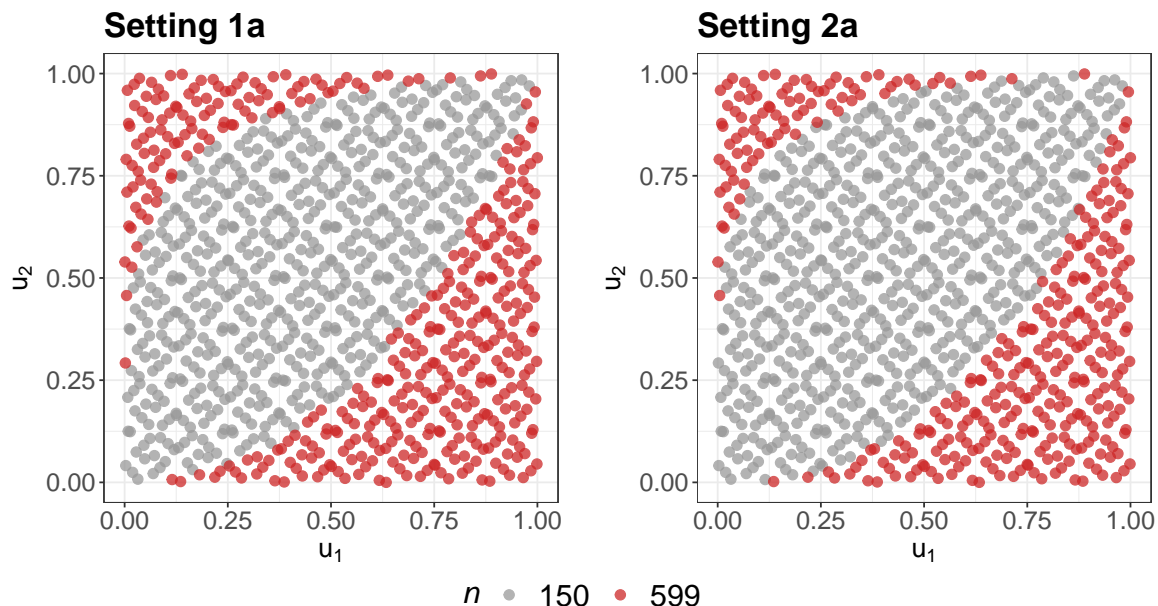


Figure C.1: Visualization of which points in  $[0, 1]^2$  are used to explore sample sizes  $n = 150$  (grey) and  $599$  (red) in the second iteration of the root-finding algorithm.

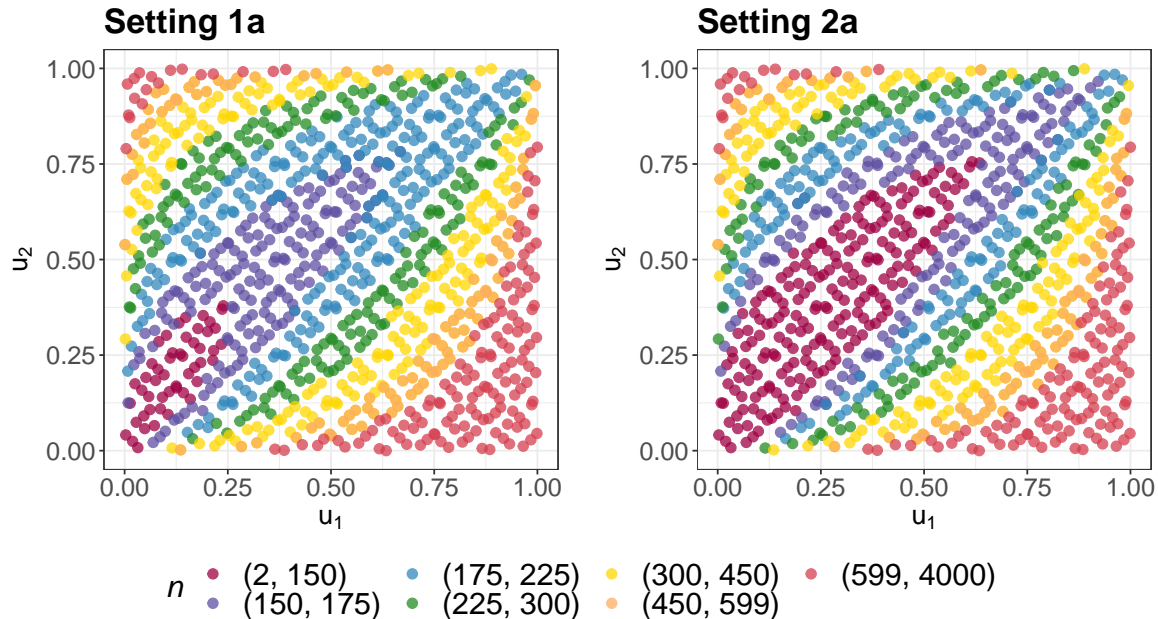


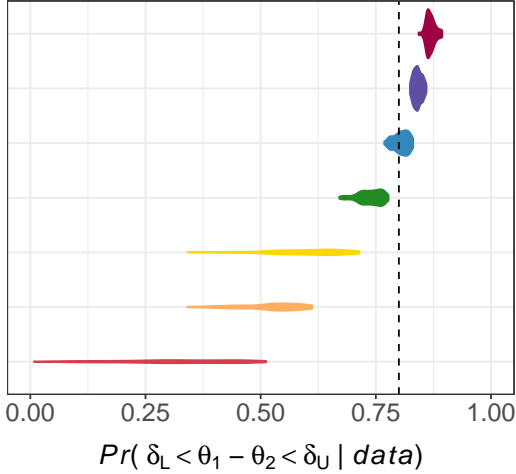
Figure C.2: Visualization of which points in  $[0, 1]^2$  are used to explore at least one  $n$  value in the various sample size ranges via the root-finding algorithm.

the sample size of  $n = 150$  in the second iteration of the root-finding procedure. Conversely, only the red points at which  $p_{300, \mathbf{u}_r, \zeta}^{\delta_U} - p_{300, \mathbf{u}_r, \zeta}^{\delta_L} < \gamma$  were used to explore the sample size of  $n = 599$ . The final sample size recommendation for Setting 2a was  $\lceil n^* \rceil = 269$ . The root-finding algorithm begins to facilitate targeted sampling in its second iteration: the plot for Setting 2a has more grey points than the one for Setting 1a to reflect its smaller sample size recommendation.

The sampling procedure becomes more targeted in subsequent iterations of the root-finding algorithm. This targeted sampling approach is visualized in Figure C.2 for both settings. For instance, only the pink points in the lower left corner of each plot assessed power for at least one sample size  $n \in (2, 150)$  when input into the root-finding procedure. We note that in subsequent iterations of the root-finding algorithm, the sample size  $n$  is noninteger, which does not present issues for our method. As in Figure C.1, the fact that Setting 2a has a smaller sample size recommendation than Setting 1a is reflected in how the points in  $[0, 1]^2$  are categorized in Figure C.2.

This targeted sampling approach is useful. Only the blue points from  $[0, 1]^2$  considered at least one sample size  $n \in (175, 225)$ . These are the points for which the posterior probability in (1.4) from the main text is close to the conviction threshold  $\gamma = 0.8$ . Figure C.3 visualizes the sampling distribution of posterior probabilities for  $n = 200$  conditional on the categorizations from Figure C.2. It is wasteful to use the pink points to consider  $n \in (175, 225)$  because those points satisfy  $p_{n, \mathbf{u}_r, \zeta}^{\delta_U} - p_{n, \mathbf{u}_r, \zeta}^{\delta_L} = \gamma$  for some sample size  $n \in (2, 150)$ . Based on Lemma 1, the posterior probabilities for the pink points for  $n \in (175, 225)$  should therefore be much larger than  $\gamma$ . This result is confirmed by comparing the pink densities to the

**Setting 1a:  $n = 200$**



**Setting 2a:  $n = 200$**

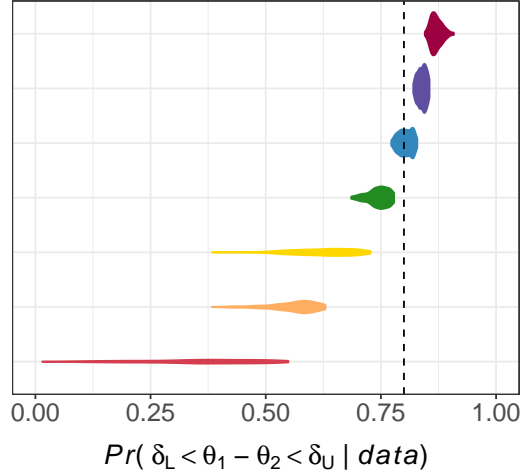


Figure C.3: Violin plots for the sampling distribution of posterior probabilities corresponding to  $n = 200$  conditional on the coloured categorization of points in  $[0, 1]^2$  from Figure C.2. The dotted vertical line is at  $\gamma = 0.8$ .

dotted vertical lines at  $\gamma = 0.8$  in Figure C.3. By similar logic, it is wasteful to consider the red points for  $n \in (175, 225)$  since the posterior probabilities for those points will be much smaller than  $\gamma$ .

In Figure C.2, the sample size categories were created to exclude most sample sizes from the first few iterations of the root-finding algorithm. This categorization limits the number of points in  $[0, 1]^2$  that belong to more than one of the seven categories for clearer visualization. We emphasize that these categories are not used in our power curve approximation method. Instead, they illustrate the targeted nature of how we sample from the approximate sampling distribution of posterior probabilities for each sample size  $n$  considered.

## C.2 Benefits of Quasi-Monte Carlo Methods

We now assess the impact of using Sobol' sequences with our power curve approximation method. To do so, we approximated 1000 power curves for the Bernoulli example from Appendix C.1 using Algorithm 4 with sequences from a pseudorandom number generator of length  $m = 1024$ . As in Appendix C.1, the posterior approximation methods in Algorithms 1 and 2 are considered for Settings 1a and 2a, respectively. We then repeated this process using Algorithm 4 with Sobol' sequences of length  $m = 1024$ . We used the 1000 power curves corresponding to each sequence type (Sobol' and pseudorandom) to estimate power for the following sample sizes:  $n = \{80, 160, \dots, 2000\}$ . For each sample size and sequence type, we obtained a 95% confidence interval for power using the percentile bootstrap method (Efron, 1982). We then created centred confidence intervals by subtracting the mean of the 1000 power estimates from each confidence interval endpoint. The right plot of Figure C.4 depicts these results for the sample sizes  $n$  and two sequence types considered.

Figure C.4 illustrates that the Sobol' sequence gives rise to much more precise power estimates than pseudorandom sequences – particularly for sample sizes where power is not near 0 or 1. We repeated the

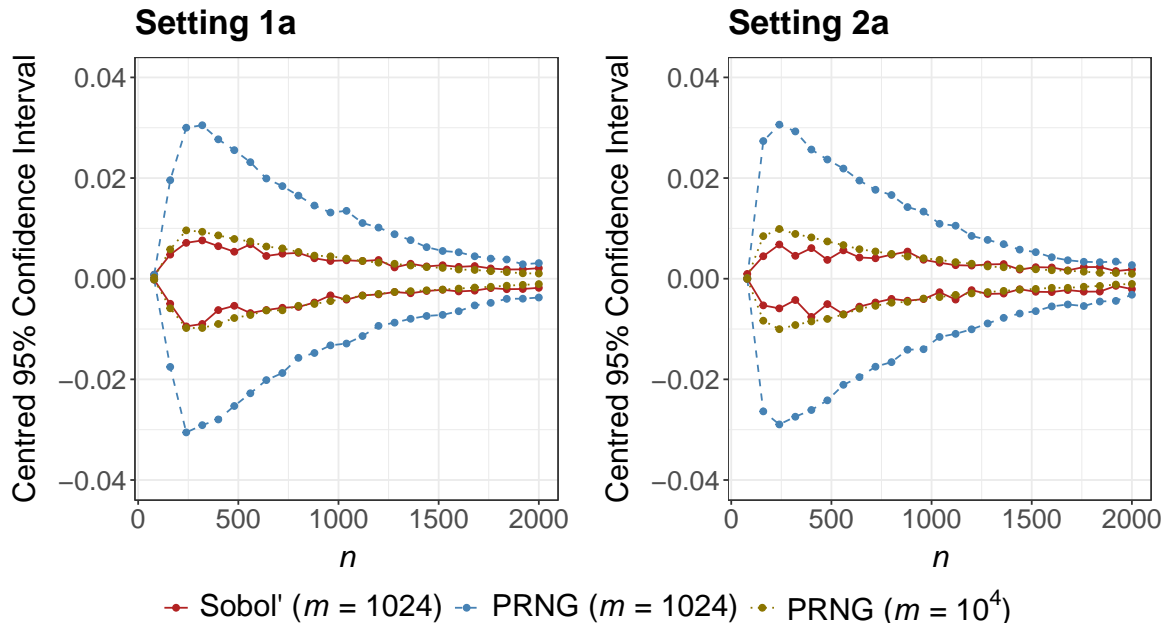


Figure C.4: Endpoints of the centred 95% confidence intervals for power obtained with Sobol’ and pseudo-random (PRNG) sequences of various lengths.

process detailed in the previous paragraph to generate 1000 power curves via Algorithm 4 with pseudorandom sequences of length  $m = 10^4$ . The power estimates obtained using Sobol’ sequences with length  $m = 1024$  are roughly as precise as those obtained with pseudorandom sequences of length  $m = 10^4$ . Similar results were observed for more extensive numerical studies. Using Sobol’ sequences therefore allow us to estimate power with the same precision using approximately an order of magnitude fewer points. Therefore, it would take roughly 10 times as long to approximate the power curve with the same precision using pseudorandom numbers in lieu of Sobol’ sequences.

## D Additional Numerical Studies

### D.1 Numerical Studies with Bayes Factors

We now compare the performance of our power curve approximation procedure for several posterior analyses with Bayes factors. To do so, we modify Settings 1a and 2a from Section 5.1 of the main text. We do not change the target power, interval  $(\delta_L, \delta_U)$ , or the prior distributions. For Setting 1a with the uninformative priors,  $Pr(\delta_L < \theta_1/\theta_2 < \delta_U) = 0.0128$ . We consider a threshold for the nonoverlapping-hypotheses (NOH) Bayes factor of  $K = 100$  for illustration. By (1.5) of the main text, this corresponds to a conviction threshold of  $\gamma = 0.5652$ . For Setting 1b with the informative priors,  $Pr(\delta_L < \theta_1/\theta_2 < \delta_U) = 0.2835$ . We consider a threshold for the NOH Bayes factor of  $K = 3$  for illustration, which corresponds to a conviction threshold of  $\gamma = 0.5428$ . This example illustrates the importance of considering the impact of the prior for  $\theta$  when choosing a threshold  $K$ .

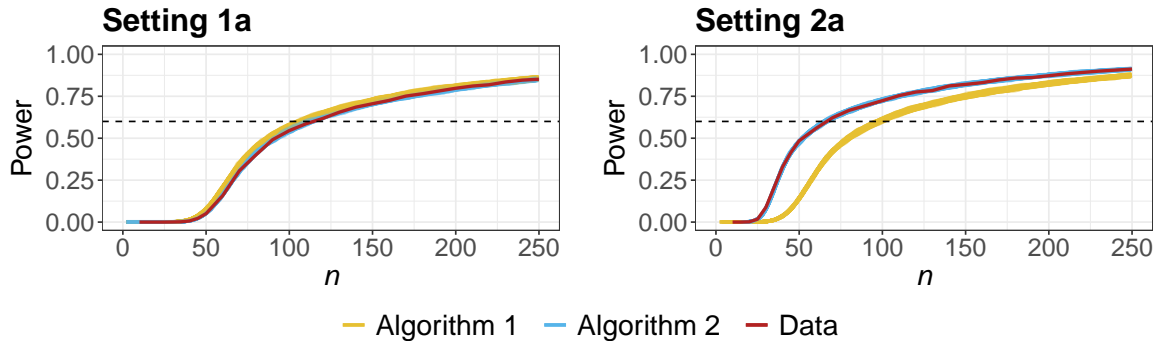


Figure D.1: 100 power curves obtained via Algorithms 1 (yellow) and 2 (blue), power curve estimated via simulated data (red), and target power  $\Gamma$  (dotted line) for Settings 1a and 2a with hypothesis tests facilitated via NOH Bayes factors.

The numerical study in this subsection was otherwise carried out using the same process as described in Section 5.1 of the main text. For each setting, we obtained 100 approximations to the power curve using Algorithm 4 with  $\zeta = \{\text{Alg. 1, Alg. 2}\}$ . The results for Settings 1a (left) and 2a (right) are depicted in Figure D.1. This numerical study supports similar conclusions as those drawn regarding Settings 1a and 2a for hypothesis tests with posterior probabilities in Figure 3 of the main text.

## D.2 Numerical Studies with Imbalanced Sample Sizes

In Section 7.2 of the main text, we acknowledge that our framework as presented in the main paper does not support imbalanced sample size determination (i.e., where  $n_2 = qn_1$  for some constant  $q > 0$ ). In this subsection, we describe how to extend our methods to allow for imbalanced sample size determination. This procedure requires practitioners to choose the constant  $q$  a priori. When  $n_1 \neq n_2$ , we use the following limiting posteriors for each group:  $\mathcal{N}(\boldsymbol{\eta}_{1,0}, \mathcal{I}(\boldsymbol{\eta}_{1,0})^{-1}/n)$  and  $\mathcal{N}(\boldsymbol{\eta}_{2,0}, \mathcal{I}(\boldsymbol{\eta}_{2,0})^{-1}/(qn))$ . To apply the multivariate delta method to obtain the limiting posterior of  $\theta = h(g(\boldsymbol{\eta}_1), g(\boldsymbol{\eta}_2))$ , both the limiting variances of  $\boldsymbol{\eta}_1$  and  $\boldsymbol{\eta}_2$  must be functions of  $n$ . We therefore treat  $\mathcal{I}(\boldsymbol{\eta}_{2,0})^{-1}/q$  as the inverse Fisher information for  $\boldsymbol{\eta}_2$  evaluated at the design value  $\boldsymbol{\eta}_{2,0}$ . This modification is also incorporated into the process to simulate maximum likelihood estimates for  $\boldsymbol{\eta}_2$  in Algorithms 1, 2, and 3 of the main text. That is, the variability in the marginal limiting distribution of  $\hat{\boldsymbol{\eta}}_{2,qn}$  is scaled to reflect the larger ( $q > 1$ ) or smaller ( $0 < q < 1$ ) sample size in the second group. Similar modifications are also made when taking the normal approximation to the posterior of  $\theta$  in (3.1), (3.2), and (3.5) of the main text. No other modifications are required to account for imbalanced sample sizes.

Lastly, we evaluate the performance of our power curve approximation procedure with several scenarios that have imbalanced sample sizes. We reuse Settings 1a and 2a from Section 5.1 of the main text. The only differences between this numerical study and the one conducted in Section 5.1 are those described in the previous paragraphs. We choose  $q = 2$  (i.e.,  $n_2 = 2n_1$ ) for this numerical study. This reflects the male

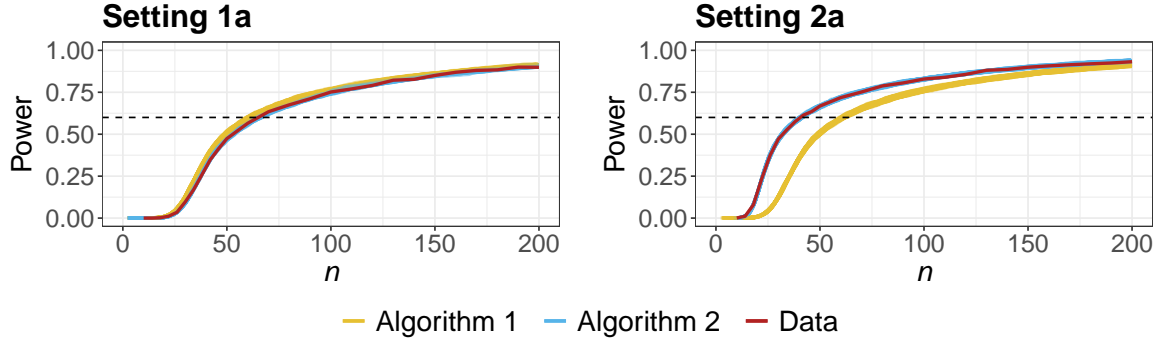


Figure D.2: 100 power curves obtained via Algorithms 1 (yellow) and 2 (blue), power curve estimated via simulated data (red), and target power  $\Gamma$  (dotted line) for Settings 1a and 2a with hypothesis tests with imbalanced sample sizes.

( $j = 2$ ) provider group having more observations than the female ( $j = 1$ ) one in the motivating example from Section 2 of the main text. For each setting, we obtained 100 approximations to the power curve using Algorithm 4 with  $\zeta = \{\text{Alg. 1, Alg. 2}\}$ . These results are depicted in Figure D.2. We again reach similar conclusions as those drawn for Settings 1a and 2a using Figure 3 of the main text.

## References

- Efron, B. (1982). *The Jackknife, the Bootstrap and Other Resampling Plans*. SIAM.
- Gelman, A., J. B. Carlin, H. S. Stern, D. B. Dunson, A. Vehtari, and D. B. Rubin (2013). *Bayesian Data Analysis*. CRC press.
- Lehmann, E. L. and G. Casella (1998). *Theory of Point Estimation*. Springer Science & Business Media.
- van der Vaart, A. W. (1998). *Asymptotic Statistics*. Cambridge Series in Statistical and Probabilistic Mathematics. Cambridge University Press.